

POLITECNICO DI TORINO

MASTER OF SCIENCE THESIS

Haptic Sensing in Teleoperated Surgery



Supervisor: **Prof. Alessandro Rizzo (Politecnico di Torino)**

Prof. Elena De Momi (Politecnico di Milano)

Instructor: **Ph.D. Hang Su (Politecnico di Milano)**

Candidate: **Hussein Mdeihly**

A thesis is submitted in partial fulfilment of the requirements for the degree of Master of Science in Mechatronics Engineering to the Department of Control and Computer Engineering at Politecnico di Torino

Politecnico di Torino

July 2019

Acknowledgements

This thesis wouldn't have been conceivable without the support and assistance of many people in so many ways. I would like to take the opportunity to express my gratitude to thank all friends and colleagues that have given me support and encouragement in my thesis work. Foremost, I would like to express my deep sincere gratitude to my supervisors, Prof. Alessandro Rizzo (Politecnico di Torino) and Prof. Elena De Momi (Politecnico di Milano) for giving me the opportunity to carry out this thesis, for their valuable guidance, encouragement and share of their research experience.

Besides my supervisors, I would like to express my gratitude to my instructor Ph.D. student Hang Su, for all the helpful thoughts that he provided during our meetings.

Finally, I am eternally grateful to my parents Sheikh Ali Mdeihly and Malak Sweidan, and my brothers Abdalla, Reda, and Mostafa, for supporting me throughout entire process, both for their endless support and patience during the entire process of my studies and especially during this master's thesis. I will be grateful forever for your love.

Abstract

Minimally Invasive Surgery (MIS) procedures, such as laparoscopy, have excited up-to-date surgery by decreasing incisions, minimizing patient recovery, time and cost. been encouraged and facilitated by teleoperated surgical robotic systems. But surgical processes using long surgical tool through small incisions on the patient abdomen lack surgeons of dexterity, sense of touch, and hand-eye coordination that they are familiar in open surgery. Robot-assisted surgery via teleoperation is favorable path to overcome these hurdles. Teleoperation refers to the remote manipulation of a slave machine by a master device over a certain distance. The teleoperation process extends the presence of the human operator and his/her ability to perform complex tasks in inaccessible environments for humans. It enables surgeons to perform a surgery on a patient located at a remote site.

Nowadays, the research in teleoperated surgery focuses on the haptic feedback and how it is important for the surgeon to feel the interaction force occurred at the remote site between the environment and the surgical tool. Haptics refers to the sense of touch. The lack of haptic feedback in teleoperated surgery is considered as a safety risk that leads to dramatic consequences as tissue damage and time consuming. Therefore, the presence of haptic feedback offers an outstanding opportunity to enhance the quality of the surgical operation.

In teleoperation system, the transmission of sensory information from the environment to the surgeon requires availability of certain sensor in the system. For this reason, the surgeon to feel the force feedback from the remote environment demands a force sensor to be mounted as close as possible to the tip of the surgical tool to directly calculates the contact (interaction) forces between the surgical tool and environment. Then the system is said to be bilaterally teleoperated.

In this thesis, we introduce a bilateral teleoperation system, which consists of a 7 degrees-of-freedom (DOF) haptic interface Sigma. 7 (Force Dimension, Switzerland) as master device and 7 DOF robotic arm lightweight robot LWR4+ (KUKA, Germany) as slave device. Furthermore, surgical tool is placed on the slave device and the 6-axis force sensor M8128C6 (SRI, China) to measure the direct interaction forces of the surgical tool with the tissue. These forces are felt by surgeon's hand on the haptic manipulator. The force sensor must be calibrated in the system where it will be used in order to have accurate measured contact forces to achieve transparency in teleoperation system. The force sensor cannot be mounted on the tip of the surgical tool to prevent electronics from entering the patient and for reasons of size and sterility. Thus, it is place between surgical tool and flange. However, in this arrangement, the force sensor during a surgical operation does not acquire only the interaction forces of the surgical tool with the tissue, but also acquires gravity force related to weight of the surgical tool, which is exerting force on the force sensor. Thus, the overall forces conveyed to haptic interface are the contact forces and the weight of the surgical tool.

The aim of this thesis is to identify (compensate) the weight of a generic surgical tool measured by force sensor during teleoperation process, to feel on the haptic interface only the contact forces of the surgical tool with the tissue. Two methods were adopted separately for estimation of tool's weight based on: Curve Fitting (CF) and Artificial Neural Network (ANN). Afterwards, calibration of multi-axis force sensor based on Singular Value Decomposition (SVD) procedure to ensure transparency in teleoperated surgery.

Experimental results demonstrated that calibration of force sensor after identifying tool gravity component by ANN enhanced robot tool identification and calibration for bilateral teleoperation. In addition, the transparency of the system was achieved by demonstrating force and position tracking of master and slave devices.

The work presented in this thesis has been done at "Medical Robotics Section (MRS) of NeuroEngineering and Medical Robotics Lab" (NearLab) in Politecnico di Milano.

Contents

Acknowledgements	ii
Abstract.....	iv
LIST OF FIGURES.....	ix
LIST OF TABLES.....	xi
List of Acronyms.....	1
1. Introduction.....	2
1.1 Teleoperation Scenario of Robotic Surgery.....	2
1.2 Force Sensing in Surgery	4
1.3 Research Motivation.....	8
1.4 Scope of the Work	8
1.5 Thesis Outline	9
2. State of the Art Review	11
2.1 Telerobotic Systems.....	11
2.2 Bilateral Teleoperation Control Schemes	17
2.3 Haptics in Surgery	19
2.4 Force Sensor Calibration	21
3. Research Methods and Equipment	23
3.1 Overview of Teleoperated Surgical System.....	23
3.2 Teleoperated Model (Hardware components)	24
3.2.1 Master device – Sigma. 7 (Force Dimension)	24
3.2.2 Slave Device – LWR4+ (KUKA, Germany).....	26
3.2.3 Force Sensor – M8128C6 (SRI, China)	27
3.3 Methodology	28
3.3.1 Workspace Mapping	28
3.3.2 Tool Gravity Identification	30
3.3.2.1 Curve Fitting based Tool Gravity Identification.....	31
3.3.2.2 ANN based Tool Gravity Identification	33
3.3.3 Force Sensor Calibration.....	35
4. Experiment Validation and Results.....	37
4.1 Calibration After CF Implementation.....	37
4.2 Calibration After ANN Implementation	39
4.3 Discussion	42

.....	44
5. Conclusion and Future Work.....	45
Bibliography.....	48

LIST OF FIGURES

FIGURE 1. 1 TYPICAL TELEOPERATED SURGERY ARCHITECTURE.....	4
FIGURE 1. 2 DA VINCI SURGICAL SYSTEM (SI VERSION). REPRINTED FROM (UZUNOGLU, 2012).....	5
FIGURE 1. 3 HAND CONTROL UNITS OF THE SURGEON CONSOLE AND THE OPERATIVE SCREEN. REPRINTED FROM (TALASAZ, 2012).	6
FIGURE 1. 4 COMPARISON OF THE DEXTERITY OF THE ENDOWRIST (LEFT) WITH THAT OF HUMAN HAND (RIGHT). REPRINTED FROM (RAMOS, DE SOUZA BASTOS, & KIM, OBESITY AND DIABETES: NEW SURGICAL AND NONSURGICAL APPROACHES, 2015).....	7
FIGURE 1. 5 THE HUMAN OPERATOR SENDS COMMANDS TO SLAVE ROBOT (RIGHT) BY CONTROLLING THE MASTER DEVICE (LEFT). SURGICAL TOOL ATTACHED TO DISTAL PART OF THE FORCE SENSOR, PLACED BETWEEN FLANGE AND SURGICAL TOOL PROVIDING THE INTERACTION FORCES BETWEEN SURGICAL TOOL AND TISSUE..	9
FIGURE 2. 1 (LEFT) RAYMOND C. GOERTZ DEMONSTRATING HIS MECHANICAL SLAVE-MASTER MANIPULATOR DEVICE. (RIGHT) RAYMOND IN THE EARLY 1950 HANDLING RADIOACTIVE MATERIAL USING ELECTRICAL AND MECHANICAL TELEOPERATORS. REPRINTED FROM (PEPE, 2018).	12
FIGURE 2. 2 TELEROBOTIC SYSTEM CRL MODEL M2 DEVELOPED BY OAK RIDGE NATIONAL LABORATORY AND USED BY NASA IN DEEP SPACE ASSEMBLY APPLICATIONS. REPRINTED FROM (TREVELYAN, KANG, & HAMEL, 2008).	12
FIGURE 2. 3 JPL ADVANCED TELEOPERATION (ATOP) SYSTEM CONTROL STATION. REPRINTED FROM (NIEMEYER, PREUSCHE, & HIRZINGER, 2008).	13
FIGURE 2. 4 ROTEX—THE FIRST REMOTELY CONTROLLED SPACE ROBOT FLEW WITH SHUTTLE COLUMBIA IN 1993. REPRINTED FROM (HIRZIGNER, SPORER, SCHEDL, & BUTTERFAB, 2002).	14
FIGURE 2. 5 GRAPHIC OPERATION OF LINDBERGH. REPRINTED FROM (NIEMEYER, PREUSCHE, & HIRZINGER, 2008).	15
FIGURE 2. 6 ZEUS ROBOTIC SURGICAL SYSTEM. (LEFT) SURGICAL CONSOLE; (RIGHT) ROBOTIC ARMS. ADAPTED FROM (AIDAN & BECHARA, 2017).	16
FIGURE 2. 7 SURGEON OPERATING THE ROBOTIC CONSOLE IN NEW YORK TO REMOVE THE GALL BLADDER OF A PATIENT IN FRANCE. REPRINTED FROM (MARESCAUX, ET AL., 2001).	16
FIGURE 2. 8 ZEUS ROBOTIC ARMS AT THE REMOTE SITE IN STRASBOURG. REPRINTED FROM (MARESCAUX, ET AL., 2001).	17
FIGURE 2. 9 TELEOPERATION MODEL. ADAPTED FROM (KUCHENBECKER, 2006).....	18
FIGURE 2. 10 POSITION-POSITION CONTROL SCHEME. ADAPTED FROM (KUCHENBECKER, 2006)	18
FIGURE 2. 11 POSITION-FORCE CONTROL SCHEME. ADAPTED FROM (KUCHENBECKER, 2006).....	19
FIGURE 3.1 OVERVIEW OF TELEOPERATED SURGICAL ROBOT CONTROL SYSTEM.....	23
FIGURE 3.2 HAPTIC DEVICE SIGMA. 7. REPRINTED FROM (FORCE DIMENSION, 2010).....	25

FIGURE 3.3. KUKA LIGHTWEIGHT ROBOT 4+ (LWR4+) WITH KUKA ROBOT CONTROLLER (KRC) AND KUKA TEACH PENDANT. ADAPTED FROM (PENZA, 2013).	26
FIGURE 3.4 6-AXIS FORCE SENSOR (M8128C6) AND INTERFACE BOX (M8128). REPRINTED FROM (NEARLAB, 2018).	27
FIGURE 3.5 TRANSFORMATION INVOLVED IN THE TELEOPERATED SURGICAL SYSTEMS. $\mathbf{Xr} \in \mathbb{R}^m$ IS THE DESIRED CARTESIAN POSITION IN THE MASTER FRAME, WHILE $\mathbf{Xd} \in \mathbb{R}^m$ IS THE DESIRED POSITION OF THE SLAVE ROBOT. mT IS A TRANSFORMATION MATRIX FROM MASTER REFERENCE FRAME TO SLAVE REFERENCE FRAME AND IS ADOPTED TO COUPLE THE MOTION BETWEEN THE SURGICAL TOOL AND THE MASTER MANIPULATOR. oT IS A CONSTANT MATRIX BET $\{M\}$ AND $\{O\}$, WHICH DEPENDS ON THE ACTUAL SETUP OF THE PLATFORM. eT IS A TRANSFORMATION MATRIX OBTAINED FROM FORWARD KINEMATICS USING DENAVIT-HARTENBERG (D-H) NOTATION. FURTHER, AN ENDOSCOPIC CAMERA IS USED TO ENABLE THE SURGEON TO VISUALIZE THE SURGICAL OPERATION IN THE PATIENT'S ABDOMEN ON THE SCREEN AT THE LOCAL SITE. wT IS THE TRANSFORMATION MATRIX BETWEEN $\{c\}$ AND $\{w\}$, REPRESENTING TRANSFORMATION BETWEEN ENDOSCOPIC CAMERA AND THE OPERATIONAL TARGET.	30
FIGURE 3.6 FORCE SENSOR AT THE SLAVE END-EFFECTOR WITH A SURGICAL TOOL ATTACHED TO FORCE SENSOR.	31
FIGURE 3.7 TOOL GRAVITY ON THE FORCE SENSOR.	32
FIGURE 3.8 FEED-FORWARD NN ARCHITECTURE FOR THE FORCE PREDICTION.	33
FIGURE 3.9 REPRESENTATION OF ROBOT AND FORCE SENSOR REFERENCE FRAMES AND TRANSFORMATION.	35
FIGURE 3.10 FORCE SENSOR CALIBRATION.	36
FIGURE 4.1 HANDS-ON MOTION OF ROBOT FOR DATA COLLECTION OF ORIENTATION ANGLES AND FORCE SENSOR MEASUREMENT IN FREE MOTION.	38
FIGURE 4.2 REAL AND ESTIMATED TOOL GRAVITY COMPONENT.	38
FIGURE 4.3 REAL AND ESTIMATED TOOL GRAVITY COMPONENT WITH DIFFERENT AMOUNT OF DATA.	38
FIGURE 4.4 HAND-FORCE APPLIED BY MEDICAL STAFF IN DIFFERENT POSES.	39
FIGURE 4.5 FORCE SIGNALS OF ROBOT AND CALIBRATED SENSOR.	39
FIGURE 4.6 THE COMPARISON RESULTS BETWEEN THE PREDICTED RESULTS BY ANN MODEL (30 NEURONS) AND THE REAL FORCES ON THE TRAINING DATASET.	41
FIGURE 4.7 THE COMPARISON RESULTS BETWEEN THE PREDICTED RESULTS BY ANN MODEL (30 NEURONS) AND THE REAL FORCES ON THE TESTING DATASET.	41
FIGURE 4.8 CALIBRATION OF FORCE SENSOR AFTER TOOL GRAVITY IDENTIFICATION WITH ANN.	42
FIGURE 4.9 MASTER AND SLAVE FORCES DURING FREE MOTION AND INTERACTION.	44
FIGURE 4.10 CARTESIAN POSITION ERRORS ALONG 3 AXES.	44

LIST OF TABLES

TABLE 2. 1 LOCATIONS FOR FORCE SENSING. ADAPTED FROM (TREJOS, PATEL, & NAISH, 2009)	ERROR! BOOKMARK NOT DEFINED.
TABLE 3. 1 FORCE DIMENSION SIGMA. 7 SPECIFICATIONS. REPRINTED FROM (FORCE DIMENSION, 2010).....	25
TABLE 3. 2 SPECIFICATIONS OF 6-AXIS FORCE SENSOR.	28
TABLE 3. 3 OVERVIEW OF SCALING TECHNIQUES. ADAPTED FROM (RADI, 2012).....	29
TABLE 4.1 RESULTS OF NETWORK TRAINING WITH DIFFERENT NUMBER OF NEURONS IN THE HIDDEN LAYER.	40
TABLE 4.2 THE OBTAINED RMSES BY USING CF AND ANN (30 NEURONS) MODEL ON THE TRAINING SET.	43
TABLE 4.3 THE OBTAINED RMSES BY USING CF AND ANN (30 NEURONS) MODEL ON THE TRAINING SET.	43

List of Acronyms

MIS	Minimally Invasive Surgery
P-P	Position-Position control architecture
P-F	Position-Force control architecture
DoF	Degree-of-freedom
RMSE	Root mean square error
3-D	3-Dimensional
CRL	Central Research Laboratory
JPL	Jet Propulsion Laboratory
ATOP	Advanced Teleoperation system

1. Introduction

1.1 Teleoperation Scenario of Robotic Surgery

Teleoperation or remote operation literally alludes to the operation of a slave machine by human operator, over a certain distance which can vary from tens of centimeters to millions of kilometers. The teleoperation procedure is used to broaden the presence of the human operator and his/her ability to perform critical tasks, potentially inaccessible or hostile environments for humans, while reducing mission costs and reducing threats on the operators. There are numerous forms of teleoperation and each has its own application and purposes. For instance, teleoperation can be used to undergo robot-assisted surgery (Okamura, 2004), to control ground vehicles (Murakami, et al., 2008), or even for underwater operations (Griffiths, 2003). In this thesis, we study the calibration of force sensor and gravity identification of the surgical tool, that ensures the transparency in bilateral teleoperation of robot-assisted surgery with haptic feedback.

Robot has been increasingly used as tele-manipulator that is controlled by a surgeon while he/she is performing a surgery, without being physically in the same location.

Surgery was classically performed using the open approach which usually requires a very big incision in order to allow for the surgeons to access the abdominal organs and remove the disease part. However, with time, in the early 1990's there was an evolution towards Minimally Invasive Surgery (MIS) with the use of endoscopic camera and very small incisions that was a major revolution and allowed surgeons to perform complex operations with tiny incisions resulting in patient's benefits such as, reduce pains, faster recovery and an early discharge. The robot doesn't do anything on its own, all the movements are controlled by surgeon. Therefore, the outcomes are driven by the expertise of the surgeon in that operation. The robot is only the tool that simplifies the operation and makes it more accurate and more precise.

Teleoperation extends the capability of human operator to manipulate objects remotely over a certain distance by providing the human operator with similar conditions as those at the remote site. This can be conceived by installing a manipulator (haptic device or joystick), called *master*, at a master site, so that the human operator can provide motion commands to the *slave* that performs a certain task. Such system is referred to as a master-slave teleoperation system. The human operator applies hand-force on the master manipulator which results in transmission of master displacements to the slave manipulator that mimics that movement.

Teleoperation assumes a key role in medical applications such as robot-assisted surgery that allows surgeons to operate the patients from remote locations (Taylor, Menciassi, Fichtinger, Fiorini, & Dario, Springer). An average current use of teleoperated robotic systems is represented by robot-assisted surgery. The Figure 1.1 shows a teleoperation system scenario. The surgeon controls the surgical tool by means of master device. From a functional point of view, a teleoperation system can be divided into two main parts: Local site and remote site. On the local site the surgeon is located with the master device that is needed to couple the surgeon with the teleoperated system. Local site is often referred in the literature as human operator (surgeon in our case) site or master site. While, at the remote site, the patient's abdomen is located with the slave robot arm. In comparison to the local site, the remote site consists of all devices and equipment such as surgical tool and sensors, which are useful to perform the surgery and sends sensory information from the remote site to the surgeon in the local site through the master device (Radi, 2012). The surgeon on the local site uses the master device and pedal switch to drive the motion of the tooltip of the surgical robot on the remote site from the actual position X to the desired one X_d . $X_r \in \mathbb{R}^3$ and $\dot{X}_r \in \mathbb{R}^3$ represent the desired position and velocity of the master device, respectively. However, $X \in \mathbb{R}^3$ and $\dot{X} \in \mathbb{R}^3$ are the actual position and velocity of the slave robot, respectively.

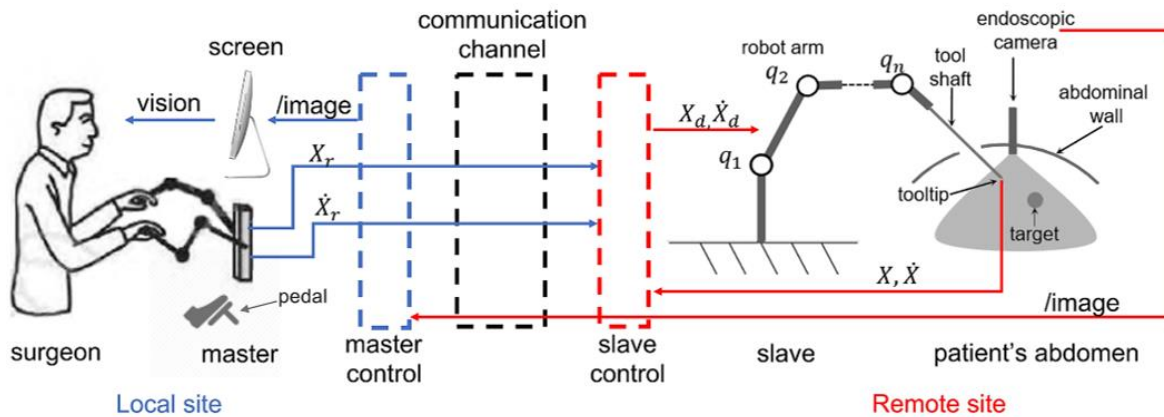


Figure 1. 1 Typical Teleoperated Surgery Architecture.

Through the recent years, several research studies have been conducted to achieve teleoperation for robot-assisted surgery, for example, the DLR MiroSurge (Tobergte, Konietzschke, & Hirzinger, Planning and control of a teleoperation system for research in minimally invasive robotic surgery, 2009). Over the last twenty years, much research has been coordinated at exploiting the advantages of incorporating robotics in medical procedures and therapy by developing suitable tools for assisting clinicians (Talasaz, 2012). Surgery was classically performed using the open approach which usually requires a very big incisions in order to allow surgeons to get access to structures or organs involved and remove the disease part (Talasaz, 2012). However, with time, in the early 1990's there was an evolution towards Minimally Invasive Surgery (MIS) with the use of endoscopic camera and very small incisions that was a major revolution and allowed surgeons to perform complex operations with tiny incisions resulting in patient's benefits such as, reduce trauma, faster recovery (Massimino & Sheridan, Human factors) and an early discharge.

1.2 Force Sensing in Surgery

The term MIS covers all surgeries with small incisions and endoscopes. The robot used in surgery is a tele-manipulator that is controlled by a surgeon, so the robot is only a tool that simplifies the operation and makes

it more accurate and more precise, whereas all the movements are controlled by surgeon. Therefore, the outcomes are driven by the expertise of the surgeon in that operation. Any high-level, planning, or cognitive decisions are made by the surgeon, while the robot oversees their mechanical implementation. The robotic surgery platform evolved as a result of the development of MIS techniques. A well-known and mostly used robot-assisted tele-surgical system is the da Vinci surgical robotic system (Fig. 1.2) from Intuitive Surgical Inc. Moreover, the robotic surgery platform allows for greater precision in a narrow field, and enables the surgeon increases dexterity, more stability, and the ability to perform more complex procedures in a small and narrow field under better visualization.



Figure 1. 2 Da Vinci Surgical System (SI version). Reprinted from (Uzunoglu, 2012).

This surgical system consists of a surgeon's console with the hand control interface (Figure 1.3) that is typically in the same room with the patient. Also, a bedside cart which is a cart where all electromechanical arms are mounted. This cart is movable and is located near the operating table according to surgery that is about to be performed. The cart is equipped with four robotic arms which play a key role in the surgical operation. One arm holds an endoscope, while the rest of the arms are attached to different instruments corresponding to incisions in the body of the patient.

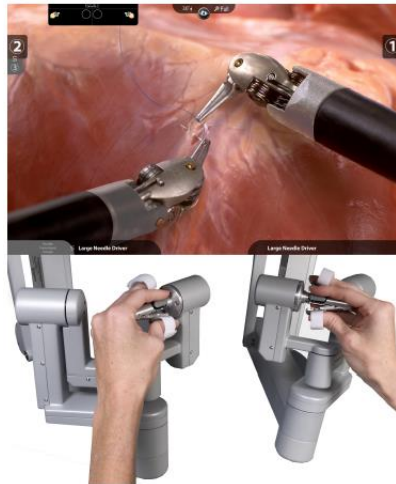


Figure 1. 3 Hand control units of the surgeon console and the operative screen. Reprinted from (Talasaz, 2012).

Besides, Da Vinci surgical systems consists also of 3-D vision system that is composed of special endoscope with dual camera for HD 3-D definition. During the operation, the console is utilized to control four interactive robotic arms using foot pedals to execute a surgery on the patient's body using EndoWrist instruments (Talasaz, 2012). The instruments exceed the natural range of the human hand; motion scaling and tremor reduction, for precise operation through small incisions (Figure 1.4).

There are a lot of advantages regarding the Da Vinci surgical system compared to non-robotic laparoscopic surgery. With the Da Vinci, the surgeon gets a 3-D visual feedback of the patient abdomen. In addition, by using a master manipulator, it is possible to scale down the motion of the surgeon leads to more precise surgery operated by the surgeon. As opposed to regular laparoscopic surgery where the surgeon remains next to the patient for the whole task, which may keep going for considerable length of time, he gets the chance to sit down by console while performing the surgery. This drives to reduction of surgical errors during a long and complicated operation.



Figure 1. 4 Comparison of the dexterity of the EndoWrist (left) with that of human hand (right). Reprinted from (Ramos, de Souza Bastos, & Kim, Obesity and diabetes: New surgical and nonsurgical approaches, 2015).

Although the Da Vinci surgical system offers dexterity and position control, it has drawback related of not transmitting haptics (force feedback) to the surgeon's side, which is considered as a considerable drawback of the Da Vinci system. Numerous studies have corresponded the lack of haptic feedback in robotic surgery to increased intra-operative surgery. For this reason, the absence of haptic feedback is a risky issue that may lead to tissue damage due to excessive forces applied by the surgeon to tissue. The results of previously conducted researches mark that haptic feedback would enhance surgeon performance and possibly patient outcomes in teleoperated surgery (Okamura, 2004).

When it comes to teleoperation for medical use, various procedures for providing force feedback to the surgeon have been estimated. The fundamental approaches are as direct force feedback, in which forces are directly applied to the surgeon's hands using enabled master manipulator, and sensory substitution, and so the force is displayed through an alternative sensory channel, such as vision or audition (Okamura, 2004).

Procedures that don't incorporate force sensing is performed with simpler and more cost-effective tools, whilst those that get benefits from for information can be performed with increased safety and efficiency (Trejos, Patel, & Naish, 2009).

A lot of haptic device are available to perceive the force feedback during robot-assisted surgery. Nowadays, the most used teleoperation master device is the Sigma. 7 (Force Dimension, Switzerland) that has 7 active degrees-of-freedom.

1.3 Research Motivation

The definitive goal of the examination of haptic feedback within the medical applications must be to come up with bilateral teleoperated system that is transparency as much as possible that can reproduce the stiffness of the environment on the remote site at the master on the local site. This strategy is beneficial in the field of teleoperated surgery. Roughly speaking, the surgeon safely and precisely controlling the haptic device during operation, can feel the interaction forces occurred at the remote site.

There are few to difficulties on the way to achieve the definitive goal. The force sensing part. Setting up a teleoperation system with a robot equipped with a 6-axis force sensor and implement the system with a haptic device to check its performance in terms of transparency and see what can be performed to optimize it performance.

Building up a teleoperation system with haptic feedback means we must use an appropriate haptic device for our system to check if this feedback will contribute in a positive way to the teleoperation system implemented for teleoperated surgery. This thesis will implement a master-slave system and test operator's experience to evaluate the transparency in the presence of haptic feedback.

1.4 Scope of the Work

When surgeon performs teleoperated surgery, he/she wants to feel as directly connected to the remote site. The force feedback transmitted to the

haptic device, enhances surgeon's performance in terms of completion of a given task (Massimino & Sheridan, Human factors), accuracy (Pacchierotti, Chinello, Malvezzi, Meli, & Prattichizzo, Springer) and the mean applied force (Wagner, Howe, & Stylopoulos, 2002) by letting the surgeon feel as if his/her own hands are in contact with patient's organ. As a result, the haptic device and the force sensor plays a major role. The force sensor must be located between flange and surgical tool to get direct measurements of interaction forces. For this reason, force sensor calibration is executed so that the surgeon perceives the real interaction force from the remote site.

However, during surgical operation, force sensor does not only feel the interaction forces, but also the gravity force due to the weight of the surgical tool, which is exerting force on the force sensor. Hence, in this case, the total force acquired by the force sensor is due to the interaction force and weight of the tool.

The scope of the presented thesis is to perform tool gravity identification to compensate the force that is present due to the weight of the generic tool, in order to have only the interaction forces acquired by the force sensor because these forces are of our interest. Besides, calibration of force sensor is implemented so that it measures accurate forces and lead to achieve transparency in teleoperated surgery.



Figure 1.5 The human operator sends commands to slave robot (right) by controlling the master device (left). Surgical Tool attached to distal part of the force sensor, placed between flange and surgical tool providing the interaction forces between surgical tool and tissue.

1.5 Thesis Outline

The thesis is outlined as follows:

- Chapter 2 shows the bilateral teleoperation control schemes, and the role of haptics in surgery, and summarizes the literature review of force sensor calibration.
- Chapter 3 introduces the hardware components used in the teleoperation system, and the developed methods adopted for tool gravity identification and force sensor calibration, with the performed analysis.
- Chapter 4 shows the experiment validation and results of the proposed methodology with KUKA LWR4+ robot.
- Chapter 5 concludes the thesis by summarizing the most important insights and contributions of the presented work. It also delineates avenues for future work.

2.State of the Art Review

2.1 Telerobotic Systems

Teleoperation appreciates a rich history dating back to nuclear research conducted by Raymond C. Goertz in the early 1940's with the first built master-slave system while working at Argonne National Laboratory, for operators to handle highly radioactive material from behind shielded walls. The operator could monitor the undertaking scene through radiation resistant viewing ports in the wall. With the earliest frameworks, the teleoperation system was electrical, and the operator used an array of on-off switches to control the motion of the slave. The first teleoperation system was fully mechanical. Without providing any force reflection (rich feel of real surfaces), these manipulators were “slow and somewhat awkward to operate”, leading Goertz to build pairs of mechanically linked master-slave robots connected by means of gears, linkages, and cables, which in turn allowed the operator to use natural hand motions and transmitted forces and vibrations through the connecting structure (Niemeyer, Preusche, & Hirzinger, 2008). The mechanical connection restricted the distance between the operator and environment and required the use of kinematically identical devices, see Figure 2.1. Later at the beginning of 1952, Goertz recognized the worth of electrically coupled master-slave manipulators and established examination of modern telerobotics and bilateral force-reflecting positional servos (Goertz & Bevilacqua, 1952).

The initial telerobotic system implemented force feedback while separating master and slave electronics was the Central Research Laboratory (CRL) model M-2 of 1982, shown in Figure 2.2. This system was jointly developed with the Oak Ridge National Laboratory (ORNL) for a broad area of demonstration tasks including military, space or nuclear applications. The mechanical systems including motors and amplifiers were designed and fabricated by CRL, while the control system and system software were developed by ORNL. Model M-2 was used and tested in deep space assembly applications.

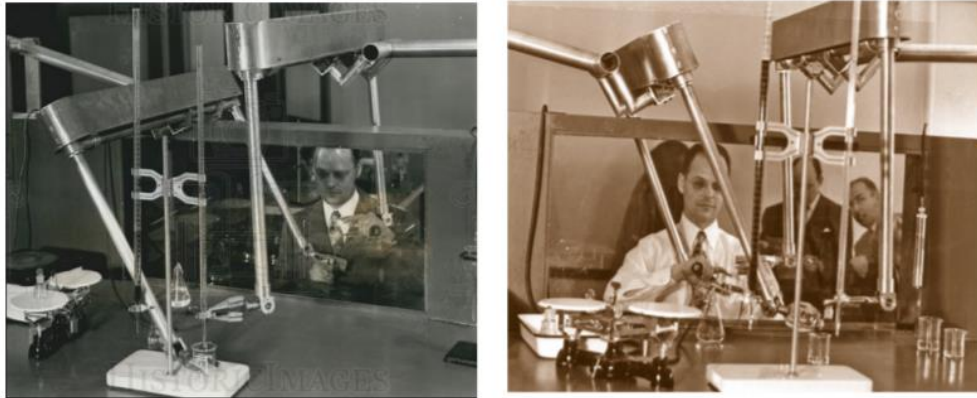


Figure 2.1 (left) Raymond C. Goertz demonstrating his mechanical slave-master manipulator device. (right) Raymond in the early 1950 handling radioactive material using electrical and mechanical teleoperators. Reprinted from (Pepe, 2018).

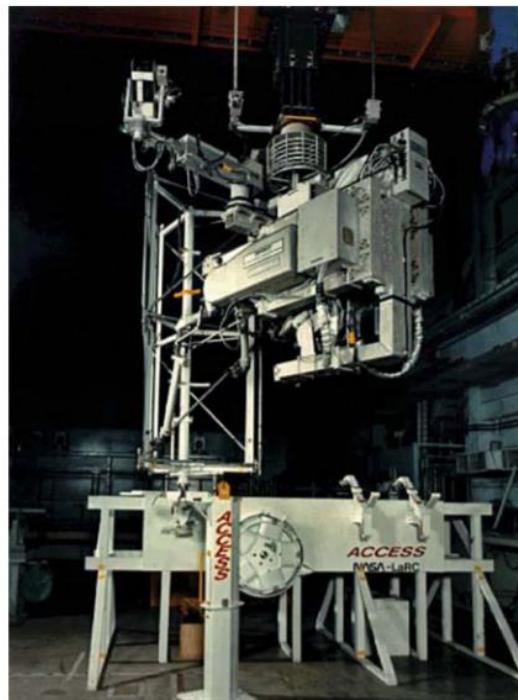


Figure 2.2 Telerobotic system CRL Model M2 developed by Oak Ridge National Laboratory and used by NASA in deep space assembly applications. Reprinted from (Trevelyan, Kang, & Hamel, 2008).

In the field of space applications, a dual-arm force reflecting telerobotic system was developed by *Bejczy et al.* at the Jet Propulsion Laboratory (JPL) to expand the two-handed manipulation capabilities of a human operator to remote places. In this process, for the first time in history, kinematically and dynamically different master and slave systems were used, requiring control in Cartesian space coordinates. Figure 2.3 exhibits the master local control station with its two back-drivable hand controllers. This system was adopted for simulating teleoperation in space.



Figure 2.3 JPL Advanced Teleoperation (ATOP) system control station. Reprinted from (Niemeyer, Preusche, & Hirzinger, 2008).

In the 1980's and 1990's, the purpose of research motivation on teleoperation systems expanded beyond the scope of nuclear power activities and became an active area of research and development in many different fields that include medicine, military and space applications. Commercial haptic devices, e.g., the Phantom device (Massie & Salisbury, 1994) were presented boosting research activities in haptic applications and virtual reality.

In early 1993 for the first time in the history of space flight, a small multisensory robot was flown in space with Spacelab-Mission D2 on board the Space Shuttle Columbia, as shown in Figure 2.4. Robot technology experiment (ROTEX) is the first remotely controlled space robot by means of local sensory feedback, predictive displays, and teleoperation (Hirzinger, Brunner, Dietrich, & Heindl, 1993). *Hirzinger et al.* mentioned that “In ROTEX the loop delays varied from 5-7 sec,” thus it was not possible to incorporate force feedback in the control loop.

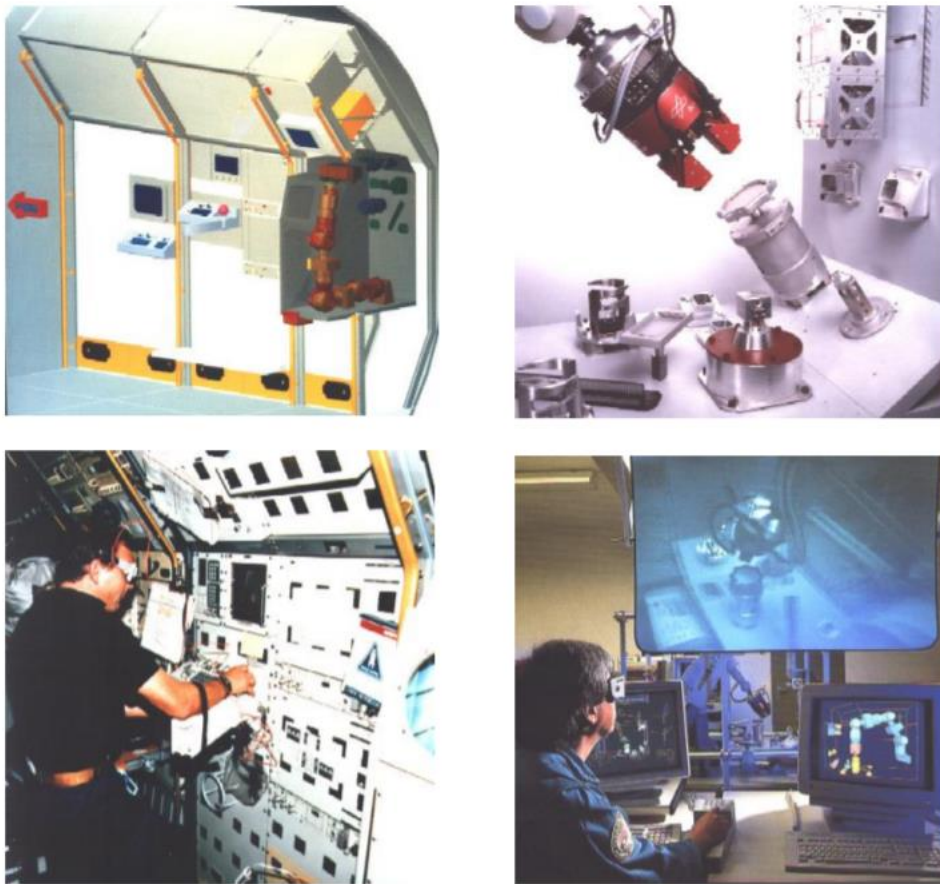


Figure 2.4 ROTEX—the first remotely controlled space robot flew with Shuttle Columbia in 1993. Reprinted from (Hirzinger, Sporer, Schedl, & ButterfaB, 2002).

In 2001, the first transatlantic surgical procedure was demonstrated, appropriately dubbed the Lindbergh operation (Figure 2.5). Later, Computer

Motion showed the feasibility of telerobotic systems even in the delicate field of surgery (Marescaux, et al., 2002). A surgeon with his assistant were in New York (USA), while other doctors were in Strasbourg (France) hospital, ready to intervene if necessary. The surgeon in New York used a ZEUS robotic surgical system (Figure 2.6) to perform a laparoscopic cholecystectomy (removal of the gall bladder using a minimally invasive procedure) across a round-trip distance of over 14,000 km. on a patient located in Strasbourg, as displayed in Figures 2.7 and 2.8. However, this system did not incorporate force feedback, so the surgeon had to rely only on visual feedback.

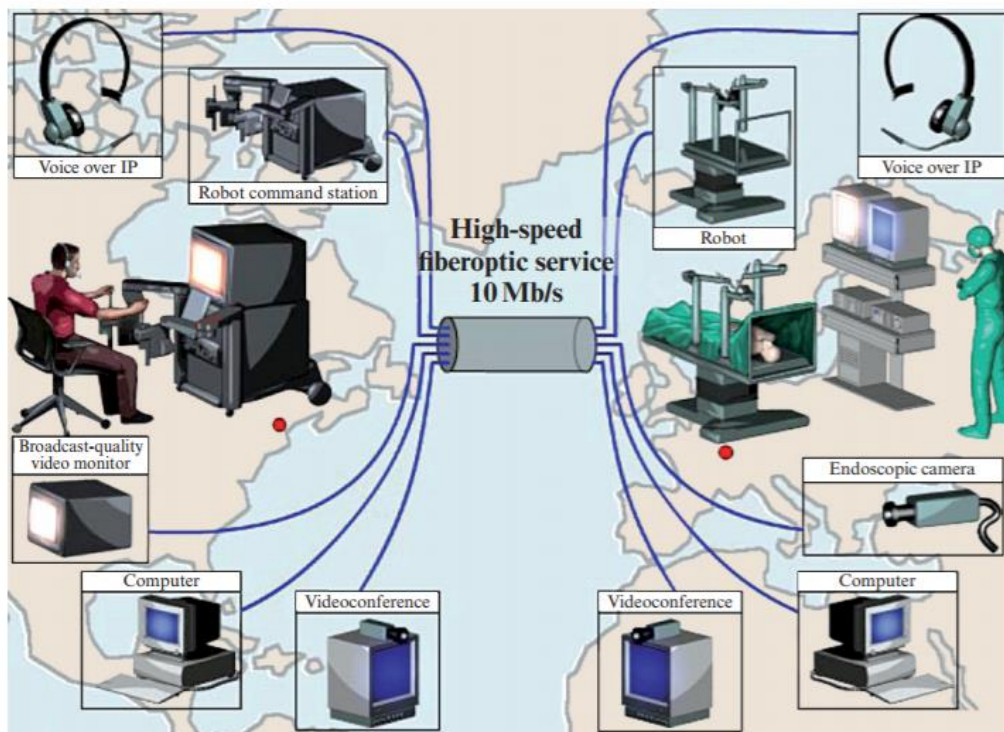


Figure 2.5 Graphic operation of Lindbergh. Reprinted from (Niemeyer, Preusche, & Hirzinger, 2008).

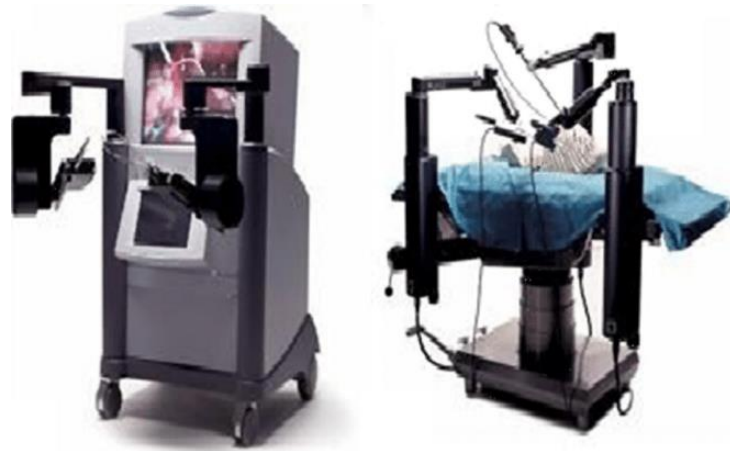


Figure 2.6 ZEUS robotic surgical system. (left) Surgical console; (right) robotic arms. Adapted from (Aidan & Bechara, 2017).



Figure 2.7 Surgeon operating the robotic console in New York to remove the gall bladder of a patient in France. Reprinted from (Marescaux, et al., 2001).

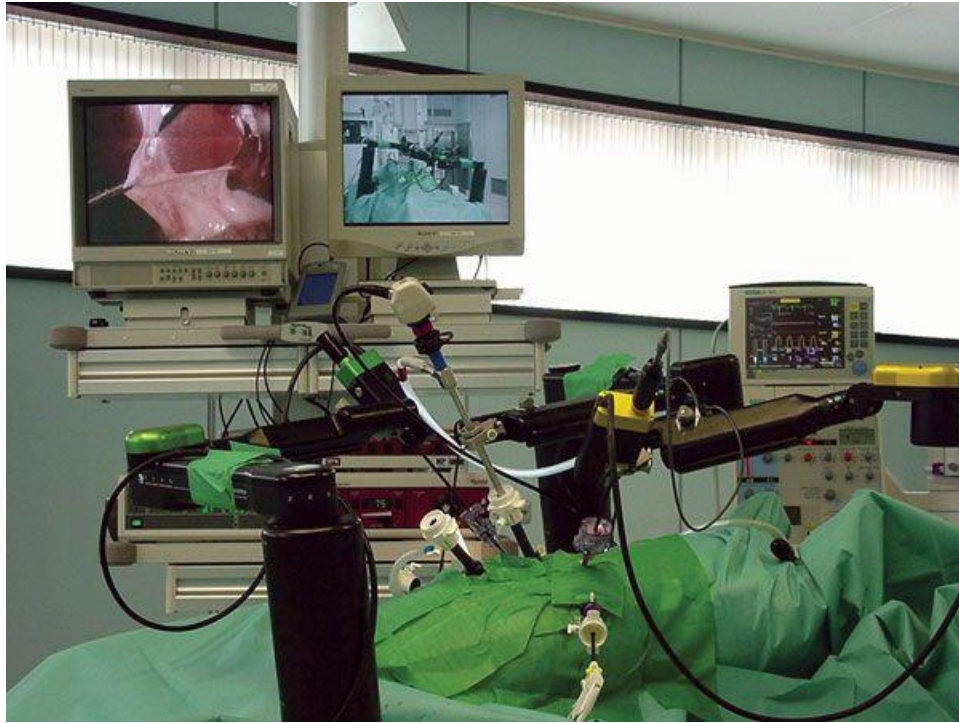


Figure 2.8 ZEUS robotic arms at the remote site in Strasbourg. Reprinted from (Marescaux, et al., 2001).

2.2 Bilateral Teleoperation Control Schemes

Bilateral teleoperator is generally referred as a system composed of five interconnected subsystems: Human operator, master device, communication channel, slave device, and environment. As illustrated in Figure 2.9, a *human operator* at the local site exerts forces on a *master device* connected through *communication channel* to a *slave device* that interacts with an *environment* at the remote site. In teleoperation system, the human operator gives input by applying hand force on the master device, while the slave device follows the commands and either sends sensor data as visual and audio or haptic feedback from the slave sensors (Li, Cox, Diftler, Shelton, & Rogers, 1996).

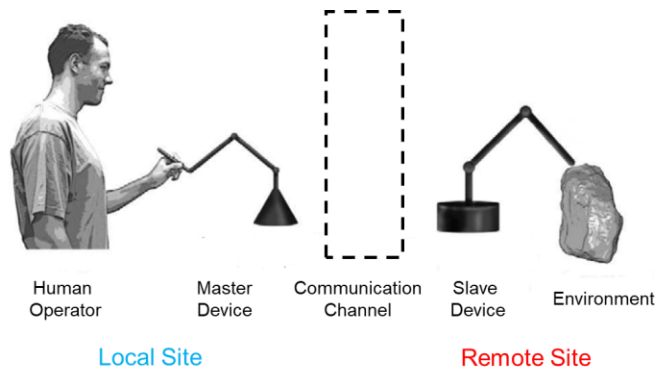


Figure 2.9 Teleoperation Model. Adapted from (Kuchenbecker, 2006).

The choice of transmitted signals marks whether the teleoperation system is *unilateral* or *bilateral*. In *unilateral teleoperation*, the signals are transmitted in one direction, from local site to remote site. However, if the signals are transmitted in both directions, then the teleoperation system is called *bilateral teleoperation system*. The transmitted signals can be in the form of either position or force. Based on the signal exchanged, the architecture can be Position-Position (P-P) (Figure 2.10), or Position-Force (P-F) (Figure 2.11).

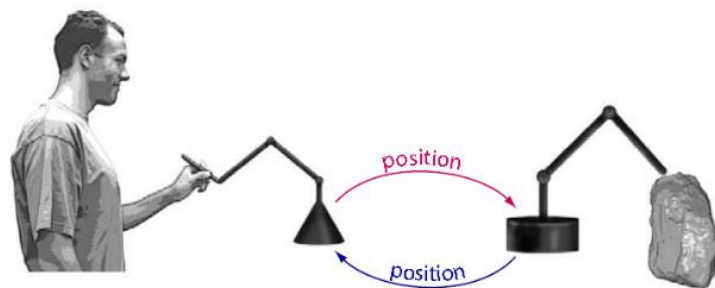


Figure 2.10 Position-Position Control Scheme. Adapted from (Kuchenbecker, 2006)

P-P architecture is the most basic bilateral controller, no force sensor measurements. As displayed in Figure 2.10, the only transmitted signals are only the positions of master and slave devices. The controller minimizes the and the controller tries to minimize the difference between the master (haptic device) and slave (robot) end-effector positions, and so reflecting a force proportional to this difference to the human operator once the slave interacts with environment. However, the lags between the master and

slave position movements will lead to large reaction forces to be reflected to the human operator (Heck, Saccon, Beerens, & Nijmeijer, 2018).

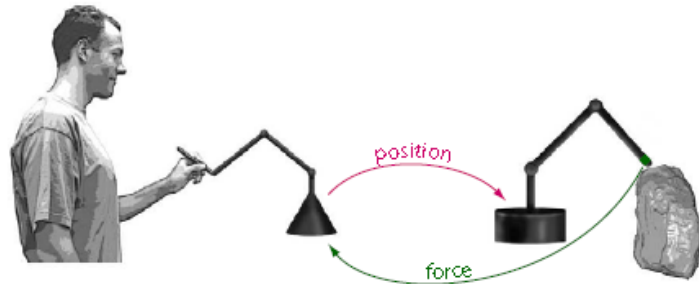


Figure 2.11 Position-Force Control Scheme. Adapted from (Kuchenbecker, 2006)

In P-F architecture, the transmitted signals, as shown in Figure 2.11 are position from master to slave and force is fed back to the human operator through the master device. In this case, a force sensor is needed to measure the interaction forces between the slave device and the environment, while the slave follows the position of master device. In terms of force reflection, this architecture seems to have more potential than the previous one, but when the slave contacts the environment, the architecture switches from unilateral to bilateral and this causes contact instabilities (Heck, Saccon, Beerens, & Nijmeijer, 2018).

2.3 Haptics in Surgery

Haptics literally refers to the sense of touch, which is one of the human senses. In teleoperated surgical system, haptics involves the reflection of the interaction between the surgical tool and tissue to the surgeon through a haptic interface. The objective of haptics in robot-assisted surgery is to ensure transparency, in which the surgeon can feel as directly connected to the remote environment (Talasaz, 2012). Consequently, it requires sensors to acquire force and touch information, and haptic manipulators to display the information to the surgeon. Haptic feedback is generally divided into two different classes: Tactile and Kinesthetic (force). Force feedback in robot-assisted surgery allows surgeons to operate a surgery as if his/her hands were in contact with the patient organs, without being physically in the same location. Thus, the ideal case would be when the forces encountered by the surgeon are exactly equal to the interaction forces occurred at the remote site between surgical tool and tissue. As a result, the surgeon would feel as directly connected to the remote environment;

the system is transparent. For some applications, visual and auditory cues may be enough as tactile substitution, but for some others there are limitations such as worsening of performance in manipulation, and sense of presence. Several studies reveal that lack of haptic feedback can increase the chances of inter-operative injury during surgery (Frith & Frith, 1974) and requires greater mental concentration from surgeon to complete a task.

No matter force feedback increases or not the surgical precision and outcome in robot-assisted surgery procedures is still under discussion, numerous studies recently confirm that the haptic feedback can enhance the performance of the surgery in terms of tissue discrimination, and completion of surgical task (De Lorenzo, 2012). For this reason, huge number of studies have been analyzed and proposed to determine the need of haptic feedback. As a result, force sensor is required to be used in the teleoperated surgical operation in order to sense the interaction forces between the surgical tool and the tissue of patient's body. The main objective is to measure the interaction forces between the tip of the surgical tool and the tissue. Table 2.1 enumerates the different locations where forces can be sensed. Consequently, a force sensor placed at the tip the surgical tool has the best performance in the detection of the interaction forces with the environment (tissue), but it needs miniaturization, sterilizability, high insulation, modification and customization of the standard surgical tool (De Lorenzo, 2012). On the other hand, a force sensor placed far from the tool tip will not detect accurately the tool-tissue interaction forces (De Lorenzo, 2012).

Locations	Advantages	Limitations
On the near of the actuation mechanism	<ul style="list-style-type: none"> Some information is readily available, no need for sterilization or miniaturization of additional sensing elements. 	<ul style="list-style-type: none"> Affected by friction, mechanism play, backlash, gravity, and inertia within the instrument. Sensing is taking place far away from where the forces are being applied. Indirect force measurement can overestimate the grasping forces.
On shaft outside entry point	<ul style="list-style-type: none"> No constraint with respect to size. Does not necessarily to be sterilizable. 	<ul style="list-style-type: none"> Measurements are affected by forces at the trocar, so they are not a good estimate of tool-tissue interaction forces.

	<ul style="list-style-type: none"> The information is useful for the design of robotic devices or in calculating the amount of force the hands need to apply. 	
On the access channels	<ul style="list-style-type: none"> Can measure interaction forces between the tool and the tissue surrounding the tool as it enters the body in order to minimize tissue damage. 	<ul style="list-style-type: none"> Sensing elements must be sterilizable and to work in warm and humid environments.
On shaft inside the body	<ul style="list-style-type: none"> Capable of measuring kinesthetic forces acting at the tip of the tool. 	<ul style="list-style-type: none"> Must be sterilizable and must work in warm and wet environments. The size of the elements is also limited to the size of the port.
On tool tip	<ul style="list-style-type: none"> Capable of measuring kinesthetic and tactile forces acting at the tip of the tool. Not affected by mechanism friction 	<ul style="list-style-type: none"> Must be sterilizable and must work in warm and wet environments Size of the elements is limited to the tool tip.

Table 2.1 Locations for force sensing. Adapted from (Trejos, Patel, & Naish, 2009)

2.4 Force Sensor Calibration

Force sensors are important source of feedback in robotic applications in which a force sensor mounted on the robot's end-effector plays a significant role in acquiring the interaction force between the surgical tool and the tissue, that is necessary to develop a reliable haptic sense (Roозbahani, 2015), avoiding generation of large impact forces. It is necessary to establish a relationship between the force signals measured and the actual forces being applied on the tissue by the surgeon while performing a surgery. For this reason, a calibration procedure needs to be executed (Trejos, Patel, & Naish, 2009) to ensure stability and accuracy of force sensing and improve surgical task quality. A lot of calibration methods are available in the literature. As one of the traditional calibration methods, least-square optimization method has been widely applied for calibration of multi-axis force sensors. However, this method is difficult since it requires large number of experimental data (Yingkun, Shilin, Xinong, & Yajum, 2012). In (Faber, et al., 2012), a calibration method was developed using a pre-

calibrated force plate. This method makes the calibration method easier but dismantling the sensor remains an issue (Roosbahani, 2015). Another method was proposed in (Florez & Velasquez, 2010) based on employing a fully calibrated sensor parallel to the sensor under calibration. Although it leads to faster calibration process, dismantling of the sensor remains an issue. These calibrations methods are not appropriate for this thesis as they ignored the gravity influence of the surgical tool and the non-linear disturbances due to the setup of the tool, which affects the force sensing accuracy in the teleoperation system.

3. Research Methods and Equipment

3.1 Overview of Teleoperated Surgical System

An overview of the developed teleoperated surgery is illustrated in Figure 3.1. The proposed teleoperation system is composed of:

- A serial redundant robot Lightweight Robot 4+ (KUKA, Germany), that is torque-controlled through the Fast Research Interface (FRI), providing a direct low-level real-time access to the robot controller.
- A master device Sigma 7 (Force Dimension, Switzerland) and a switch pedal to teleoperate the robot.
- HD endoscopic camera that provides video stream.
- 6-axis force sensor (M8128C6, SRI, China), that has the purpose of measuring the interaction force between surgical tip and tissue.

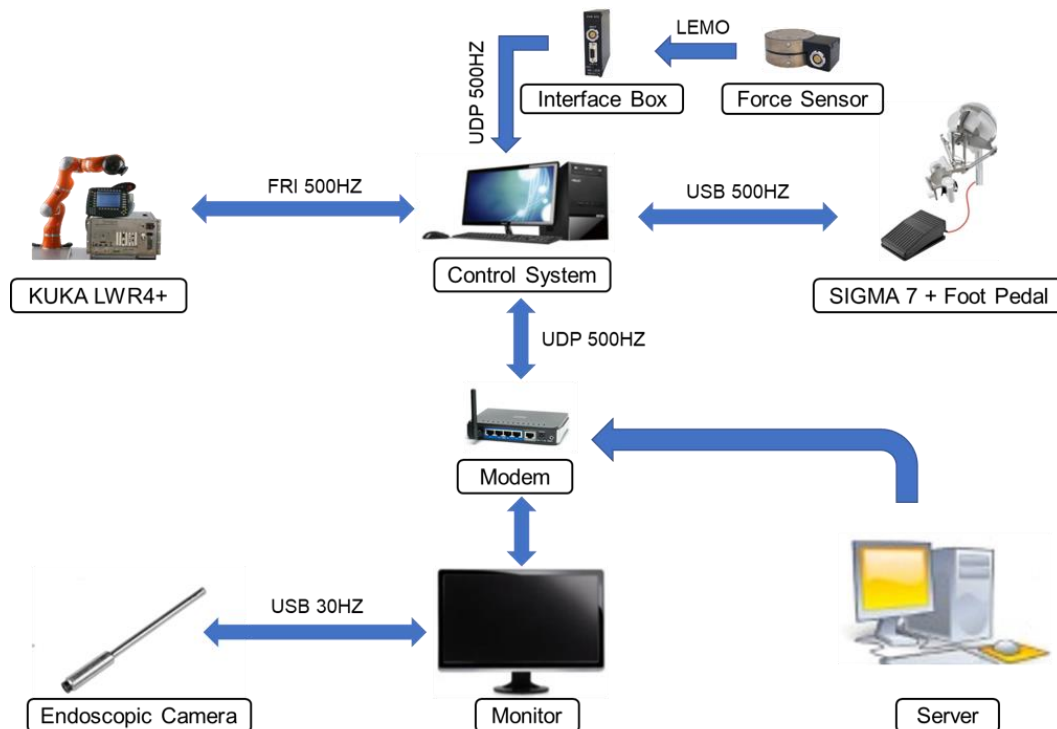


Figure 3.1 Overview of teleoperated surgical robot control system.

3.2 Teleoperated Model (Hardware components)

The proposed bilateral teleoperation system consists of a haptic device (master device) Sigma. 7 (Force Dimension, Switzerland), a slave device the Lightweight Robot LWR4+ (KUKA, Augsburg, Germany), and a 6-axis force/torque sensor (M8128C6, SRI, China) is adopted to measure the interaction force between the surgical tip and the tissue.

Slave robot LWR4+ is placed at the remote site beside a surgical table on which the surgery is performed, while the master device is on local site beside the human operator. Further, 6-axis force sensor mounted between end-effector and surgical instrument, transmits the force feedback to the human operator by measuring the interaction forces of the surgical tool with the tissue.

3.2.1 Master device – Sigma. 7 (Force Dimension)

Bilateral force-reflecting telerobotic framework requires the availability of special master devices able to display force feedback to the human operator. Various researches have affirmed that such haptic interfaces can impressively improve the performance of the teleoperation system providing the operator with adequate information about physical interaction occurring in the remote site. The master device of the bilateral teleoperation system is Sigma.7 (Force Dimension, Switzerland), shown in Figure 3.2.

The Sigma.7 is the most progressive master haptic interface ever designed by the Swiss company Force Dimension. It presents 7 active degrees-of-freedom, including high precision active grasping capability. Finely tuned to offer flawless gravity compensation, the force and torque feedback end-effector shows notable haptic behavior, approving instinctive interaction with complex haptic applications (Force Dimension, 2010). It is highly used in robotic surgery to enable the surgeon to perform a remote surgery on a patient. The electromechanical structure of the sigma.7 haptic input device involves three primary parts (Tobergte, et al., 2011): translational base, rotational wrist extension and grasping unit. Table 3.1 enumerates the specifications of the haptic device Sigma 7.



Figure 3.2 Haptic Device Sigma. 7. Reprinted from (Force Dimension, 2010).

	Translation	Rotation	Grasping
Workspace	$\varnothing 190 \times 130 \text{ mm}$	$235 \times 140 \times 200 \text{ deg}$	25 mm
Forces	20.0 N	400 mNm	$\pm 8.0 \text{ N}$
Resolution	0.0015 mm	0.013 deg	0.006 mm

Table 3.1 Force Dimension Sigma. 7 specifications. Reprinted from (Force Dimension, 2010).

3.2.2 Slave Device – LWR4+ (KUKA, Germany)

The slave device used in this thesis is serial robot arm, the Lightweight Robot 4+ (LWR4+), (KUKA, Germany), displayed in Figure 3.3.

The LWR4+ from KUKA Roboter is a 7 DoFs lightweight robotic arm, which model is supposed to be based on the human model of an arm. The main characteristics of LWR4+ Robot is specified in (Penza, 2013):

- A redundant robot (LWR4+, KUKA, Germany) which is torque-controlled through the Fast Research Interface (FRI), provides a direct low-level real-time access to the robot controller (KRC).
- It has payload capacity of 7 kg, and itself has a mass of 14 kg.
- The 7 DoFs makes the redundancy a key factor of this robot.
- Torque sensors are available in each of the seven joints.
- With its in-built sensitivity, achieved by means of the integrated sensors, the LWR 4+ is ideally suited to handling and assembly tasks.



Figure 3.3. KUKA Lightweight Robot 4+ (LWR4+) with KUKA Robot Controller (KRC) and KUKA Teach Pendant. Adapted from (Penza, 2013).

3.2.3 Force Sensor – M8128C6 (SRI, China)

The 6-axis force sensor (M8128C6) is from SRI, China, providing 3-axis force and 3-axis torque, portrayed in Figure 3.4. It is adopted to measure the interaction force between the surgical tip and tissue and achieve haptic feedback during teleoperation.

This force sensor is made of (NearLab, 2018):

- Interface Box M8128
- 1 LEMO connector
- 1 ethernet interface for Windows, Linux and Mac PC Connection
- 1 load cell
- iDAS RD debugging software



Figure 3.4 6-axis Force sensor (M8128C6) and Interface box (M8128). Reprinted from (NearLab, 2018).

The specifications of the force sensor are given in Table 3.2.

SPECIFICATIONS	
Power Supply	± 15
Overload Capacity (%F.S.)	1000
Lowest Free Air Resonant Freq. (HZ.)	750
Crosstalk-with adjustment (%F.S.)	2
Non-Linearity (%F.S.)	0.5
Hysteresis (%F.S.)	0.5
Operating Temp. Range ($^{\circ}C$)	-40 To +50

Compensated Temp. Range ($^{\circ}C$)	10 To 70
Mass (Kg)	0.41

Table 3. 2 Specifications of 6-axis Force Sensor.

The interface box M8128 supplies bridge excitation, signal conditioning, data acquisition and digital communication to the user's controller or PC via RS232, CAN Bus or Ethernet. The data rate is up to 2KHz. Besides, a 6 axis loadcell is connected to the Interface Box via a 19 pin LEMO connector.

3.3 Methodology

In the practical teleoperation applications, the master haptic device and the slave robot are different in kinematics and workspace size (Chotiprayanakul & Liu, 2009), which requires workspace mapping strategy to enable the surgeon to span the whole workspace of the slave manipulator (Mamdouh & Ramadan, 2012). In addition, its gravity terms due to the weight of the tool should be estimated and compensated during the motion to reproduce only tool-environment interaction force on the hand of the surgeon. Moreover, to achieve tool gravity identification process, two techniques have been performed: CF and ANN, separately. The performance of both techniques is compared on a same online operational procedure in terms of accuracy. Once the tool gravity force is identified, force sensor calibration using SVD is implemented to transform the force information into robot coordination frame to achieve accurate force feedback measurement from the remote site to the local site. Based on the above methodology, a final bilateral teleoperation demonstration for surgical tasks is used to verify the proposed methodology.

3.3.1 Workspace Mapping

The task of precise teleoperation of a huge workspace industrial robot utilizing a small haptic device having a limited workspace is yet a challenge, since it ought to be handled carefully without disturbing the operator perception of continuously manipulating the robot in an accurate way (Mamdouh & Ramadan, 2012) . Consequently, workspace mapping must be adopted. This issue focuses on manipulating a huge robot through its entire workspace by using a relatively small haptic device.

Workspace mapping, displayed in Figure 3.5, is performed to map the master haptic device motion trajectories into a reachable workspace for the

slave robot. To overcome this problem, a lot of scaling techniques have already been conducted in the literature (see Table 3.3).

Overview of Some Scaling Techniques		
Method	Pros	Cons
Rate Control	<ul style="list-style-type: none"> • Simple • Understandable • Infinite Workspace 	<ul style="list-style-type: none"> • No direct kinematic correspondence
Workspace Drift Control	<ul style="list-style-type: none"> • Manipulating large objects • Using small haptic device 	<ul style="list-style-type: none"> • Only virtual environments
Hybrid position/ rate control	<ul style="list-style-type: none"> • Position and rate control at once • No manual switching 	<ul style="list-style-type: none"> • Complex Implementation

Table 3.3 Overview of scaling techniques. Adapted from (Radi, 2012).

The movements executed by the surgical tool (attached at slave arm) must be equal to the movements of the haptic device end-effector in terms of rotation and translation. As shown in Figure 3.5, the slave robot is controlled by the master manipulator. To drive the end-effector position ($X \in \mathbb{R}^3$) reaching the desired position ($X_r \in \mathbb{R}^3$) from the master, an interpolation method is introduced to enable the robot to reach the desired position (X_d) smoothly:

$$X_d = -k_0(X - {}^e_m T X_r) + {}^e_m T \dot{X}_r \quad (3.1)$$

where ${}^e_m T$ is the transformation matrix from the master frame to the slave frame, $k_0 > 0$ is a positive coefficient.

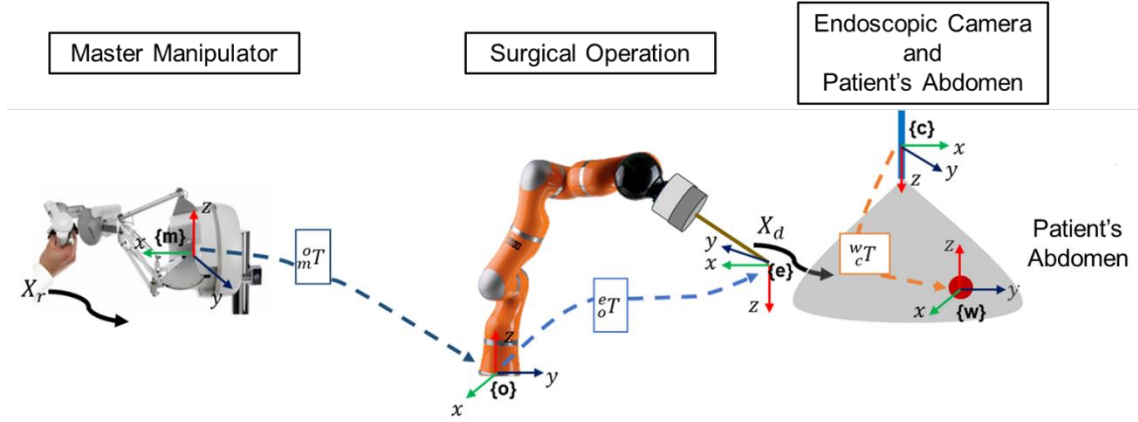


Figure 3.5 Transformation involved in the teleoperated surgical systems. $X_r \in \mathbb{R}^m$ is the desired Cartesian position in the master frame, while $X_d \in \mathbb{R}^m$ is the desired position of the slave robot. ${}^o_m T$ is a transformation matrix from master reference frame to slave reference frame and is adopted to couple the motion the motion between the surgical tool and the master manipulator. ${}^m_o T$ is a constant matrix bet $\{m\}$ and $\{o\}$, which depends on the actual setup of the platform. ${}^e_o T$ is a transformation matrix obtained from forward kinematics using Denavit-Hartenberg (D-H) notation. Further, an endoscopic camera is used to enable the surgeon to visualize the surgical operation in the patient's abdomen on the screen at the local site. ${}^w_c T$ is the transformation matrix between $\{c\}$ and $\{w\}$, representing transformation between endoscopic camera and the operational target.

3.3.2 Tool Gravity Identification

In order to transmit the interaction force of the slave robot to the surgeon, as stated previously, the force sensor is mounted between the slave end-effector and the surgical tool as portrayed in Figure 3.6. The tool is attached to the force sensor which measures the interaction force with the environment.

Since the surgical tool is located after the force sensor (Figure 3.6), there is an additional force exerted on the force sensor due to the tool's weight, which varies with the tool orientation. Hence, a problem will arise during teleoperation since the surgeon will not only perceive the interaction force with environment, but also the force exerted on the force sensor due to tool's weight. Consequently, tool gravity identification at force sensor is needed to compensate the influence of the tool weight from force sensor measurements. The force acquired by the force sensor can be expressed as follows:

$$F_S = F_{Tool\ Gravity} + F_{Interaction} \quad (3.2)$$

where $F_{Tool\ Gravity} \in \mathbb{R}^3$ is the force due to tool's weight, while $F_{Interaction} \in \mathbb{R}^3$ is the interaction forces of tool-tip and the organ tissue in the abdomen.

When the robot changes orientation, the impact of the tool's weight on the force sensor measurements varies. Thus, it is essential to consider the gravity identification depending on the end-effector pose, especially with its orientation. The relation can be modeled based on the orientation of the tool. Moreover, the interaction force acquired by the force sensor is obtained by adding compensated force to measured force by the sensor.

$$F_S = F_{Interaction} + F_{compensated} \quad (3.3)$$

where $F_{compensated} \in \mathbb{R}^3$ is the force compensated from force sensor measurements after tool gravity force is identified.

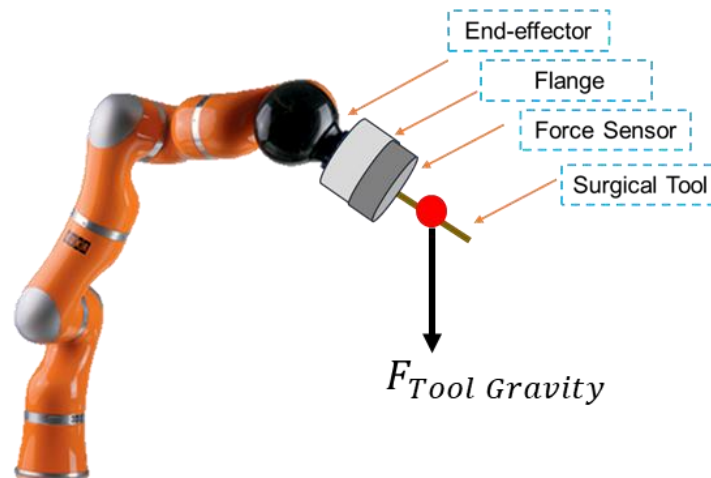


Figure 3.6 Force Sensor at the slave end-effector with a surgical tool attached to force sensor.

3.3.2.1 Curve Fitting based Tool Gravity Identification

The process of finding the equation of the curve of best fit to predict the unknown values is most known as CF. In the related regression analysis, CF uses the Least-Squares method to fit data mapping (Wen, Ma, Zhang, & Ma, 2012).

Although it is hard to find a perfect mathematical model of the surgical tool, there may be one that can approximate its behavior. The mathematical

model of the surgical tool gravity force on the force sensor output, shown in Figure 3.7, depending on the Euler angles can be defined as following:

$$F_{Tool\ Gravity} = \begin{cases} F_x = -mg * \sin(\theta_1) * \cos(\theta_2 + d) + a \\ F_y = -mg * \sin(\theta_1) * \sin(\theta_2 + d) + b \\ F_z = mg * \cos(\theta_1) + c \end{cases} \quad (3.4)$$

where F_x, F_y and F_z are the outputs of the force sensor. The unknown constants are the mass m , and the coefficient a, b , and c . Whereas, g represents gravity which is $9.8\ m/s^2$. The angles θ_1 and θ_2 are computed from the orientation angles of the tool pose. It ought to be noticed that the relation between θ_1, θ_2 and the Euler angles θ_x, θ_y , and θ_z is a mapping relation, where θ_1 is determined by θ_z while θ_2 is determined by θ_x and θ_y . However, d is a deviation error angle around z axis from the tool installation.

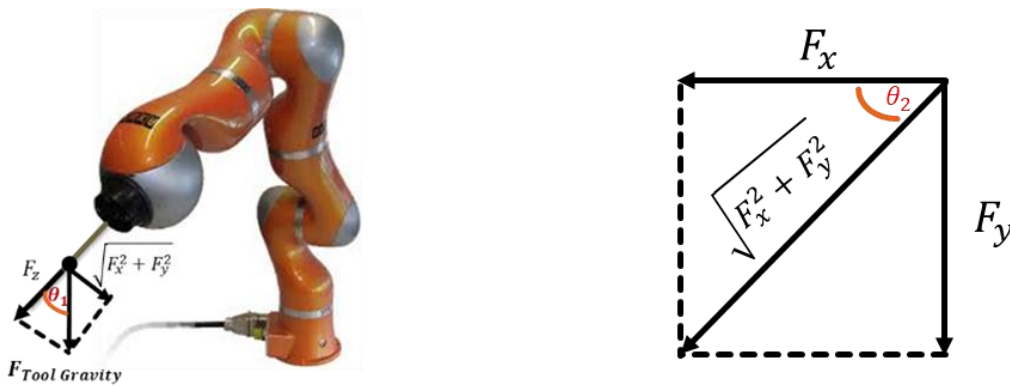


Figure 3.7 Tool Gravity on the Force Sensor.

Using CF to estimate parameters existing the linear model in (3.4) is an efficient solution. However, due to the installation of the tool in the practical application cannot be in a straight way, there should be a deviation error on θ_1 . Thus, it is difficult to project the gravity force of the tool on the force sensor with the mathematical model proposed in (3.4). As a parametric regression, the accuracy of CF relies on the prior knowledge of the mathematical system model, while it is difficult to obtain an accurate model considering the mechanical error. As a result, the precise mapping relation between the gravity and the Euler angles of the tool direction should be complex to estimate.

3.3.2.2 ANN based Tool Gravity Identification

Neural Networks (NNs) provide a new solution for the modelling of linear and non-linear curve fitting problems (Bishop & Roach, 1992). NNs have the learning capacity which can model any complex function and non-linear relationships by training the NN on a certain set of inputs to get an associated set of target outputs (Kaushik, Soni, & Soni, 1969).

As previously stated, the force mapped on the force sensor by the tool gravity depends on the orientation of end-effector. Since the regression model between the Euler angle and the force on the force sensor has been introduced and solved using CF, a feedforward back-propagation ANN with 1 hidden layer was implemented to train the regression mapping function in this paper. It is known for approximating any function, regardless of its linearity. The regression function for mapping the Euler angles to the outputs on the force sensor can be defined as:

$$F = f(\theta_x, \theta_y, \theta_z) \quad (3.5)$$

According to the input and prediction output, Figure 3.8 portrays the diagram of the proposed NN to estimate the complex relation, where the inputs θ_x, θ_y and θ_z represent Euler angles of end-effector, while F_x, F_y and F_z are the target outputs of our ANN model.

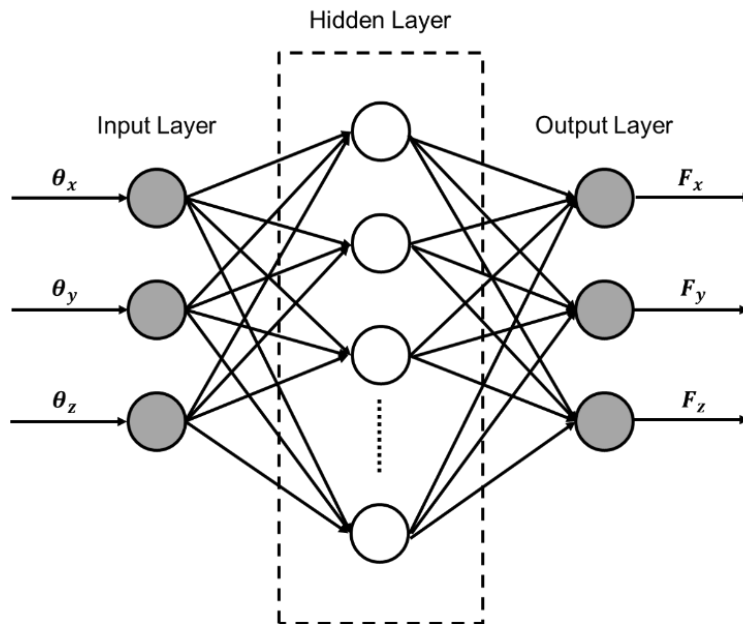


Figure 3.8 Feed-forward NN architecture for the force prediction.

The number of neurons of the hidden layer was determined by assessing the performances of the regression network. In this thesis, non-linear least squares algorithm Levenberg-Marquardt algorithm is used to calculate the maximum or minimum gradient. It has the local convergence of the Gauss-Newton method to minimize those functions and has a gradient descent method of global characteristics to look for a new search direction. The training of the neural network and the performance index is set as the mean square error. The final NN model can be written as:

$$Y = W_2 \cdot \left(\frac{1}{1 + e^{-(B_1 + W_1 X)}} \right) + B_2 \quad (3.6)$$

Where $X = [\theta_x, \theta_y, \theta_z]$ is the input matrix, $B_1 = [b_1; b_2; \dots; b_j]$ is the bias matrix of the first layer, j is the number of neurons and $B_2 \in \mathbb{R}^{3 \times 1}$ is the bias of the output layer, while $W_1 \in \mathbb{R}^{j \times 3}$ and $W_2 \in \mathbb{R}^{3 \times j}$ are the corresponding weight matrix. The initial condition of the weights and bias are initialized to small random number. In this thesis, parameters move in the opposite direction of the error to reduce the mean square error to get minimum value. The updating law to determine the weight matrix adopted the increment way. The update law of the weight is given by Gradient Descent rule using the following equation:

$$W_{i,j}(t + 1) = W_{i,j}(t) - \eta \frac{\partial L}{\partial W_{i,j}} \quad (3.7)$$

where, η is the learning rate and L is the loss function. In this work, $\eta = 0.01$. To improve the effectiveness for training the ANN model, we choose 1.05 ratio to increase learning rate and set the maximum validation failures is 6.

After generating the model, Random Data Division (*dividerand*) for the network is selected in order to allow maximum use of data for training. The data are broken into three distinct datasets: Training (70%), validation (15%), and testing (15%) sets. The training set is a set of data employed to train the model and was also used to update the neurons weights with the predefined number of iterations. The validation set is a set of data that is separate from the training set and is used to validate our model during training. One of the main reasons that we need validation set is to minimize overfitting. Besides, when the NN converged to its final configuration, the testing set was used to access its actual ability to predict force sensor outputs based on Euler angles. As a network training function, *trainlm* that updates weight and bias to acquire new knowledge according to Levenberg-

Marquardt optimization was selected to solve non-linear least squares problems.

3.3.3 Force Sensor Calibration

Force sensor is particularly significant source of feedback in robotic applications to measure forces along x , y and z axes at robot's end-effector so that increasing sensitivity of the surgeon. The success of robot-assisted surgery with haptic feedback demands accurate force tracking of the teleoperated slave robot. This requires force sensor mounted at the robot's end-effector to acquire force and touch information and fed them back to the surgeon.

To achieve the best possible transparency, force sensor should be calibrated in the system where it will be used. The SVD of a matrix is a linear algebra tool that has been successfully applied to a wide variety of domains (Papadopoulos & Lourakis, 2000). In this thesis, SVD method (Kim, Sun, Voyles, & Nelson, 2007) is adopted to figure out the transformation (calibration) matrix f_eT between slave's end-effector and force sensor, reference frames, as depicted in Figure 3.9. Further, Figure 3.10 demonstrates the input-output of our calibration method, where $F_R \in \mathbb{R}^3$ and $F_S \in \mathbb{R}^3$ are the robot and sensor forces, respectively. ${}^f_eT \in \mathbb{R}^{4 \times 4}$ is the obtained calibration matrix.

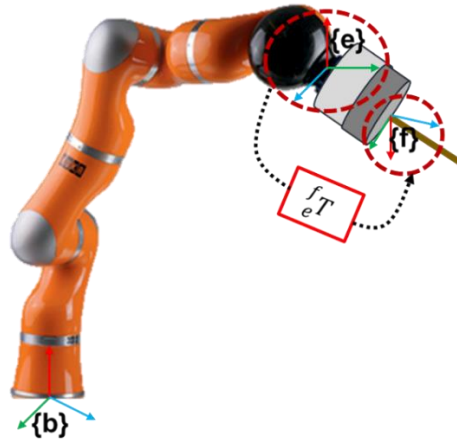


Figure 3.9 Representation of robot and force sensor reference frames and transformation.

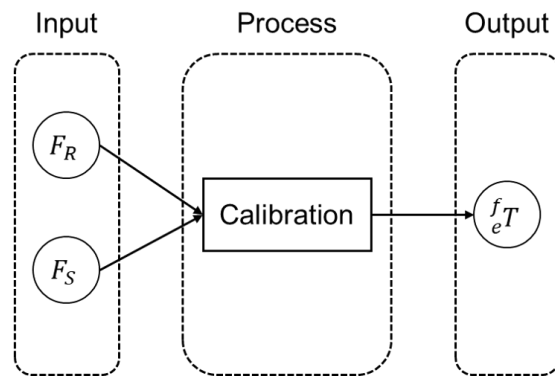


Figure 3.10 Force Sensor Calibration.

4. Experiment Validation and Results

This chapter presents the experiment validation and results of the proposed methodology evaluated with KUKA LWR4+ robot.

4.1 Calibration After CF Implementation

The first method used for tool gravity identification is CF. As mentioned in section 3, gravity identification is implemented with respect to current end-effector orientation. Thus, different amount of data was collected for estimation and validation, using hands-on control to allow the user to move the robot arm without touching the robot tool and the force sensor. as depicted in Figure 4.1. With the use of Curve Fitting Toolbox, it is possible to obtain the unknown parameter m and the coefficients a , b and c , from the first group of sampled data (41729 samples). Then, the obtained parameters are placed in the mathematical model (3.4) to predict the force on the force sensor, which is expressed as follows:

$$F_{Tool\ Gravity,estimated} = \begin{cases} F_{x,estimated} = -0.3434 * g * \sin(\theta_1) * \cos(\theta_2 + 1.401) + 0.6 \\ F_{y,estimated} = -0.3434 * g * \sin(\theta_1) * \sin(\theta_2 + 1.401) + 1.1 \\ F_{z,estimated} = 0.3434 * g * \cos(\theta_1) + 2.0 \end{cases} \quad (4.1)$$

In order to verify whether the predicted data using (4.1) fits the real measurements acquired by the force sensor, the second group was used for validation (32047 samples). The error between the real force and estimate force is analyzed. Figures 4.2 and 4.3 depict the difference between the real and estimated force along the different axis. Once the gravity force $F_{Tool\ Gravity}$ being identified by CF technique, force signals data are acquired from both robot and sensor, as shown in Figure 4.4, to perform force sensor calibration so as to couple both signals by means of SVD method. Results of calibration are exhibited in Figure 4.5.



Figure 4.1 Hands-on motion of robot for data collection of orientation angles and force sensor measurement in free motion.

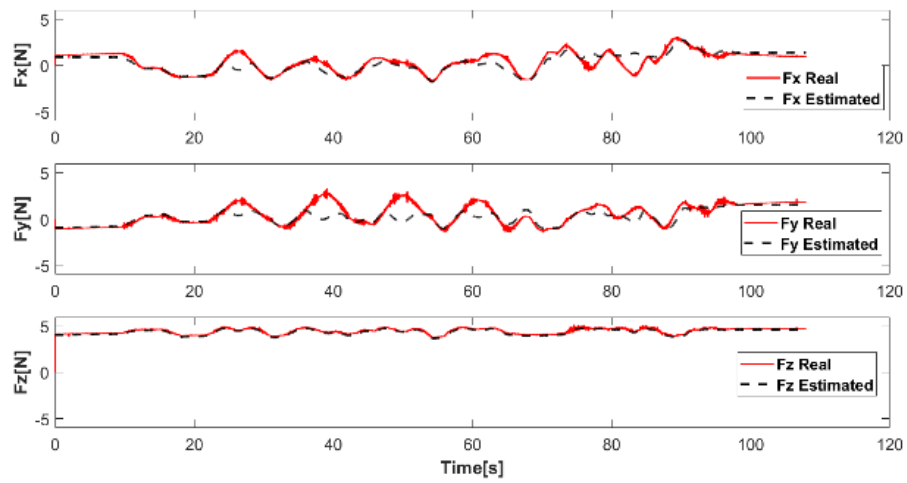


Figure 4.2 Real and Estimated Tool Gravity component.

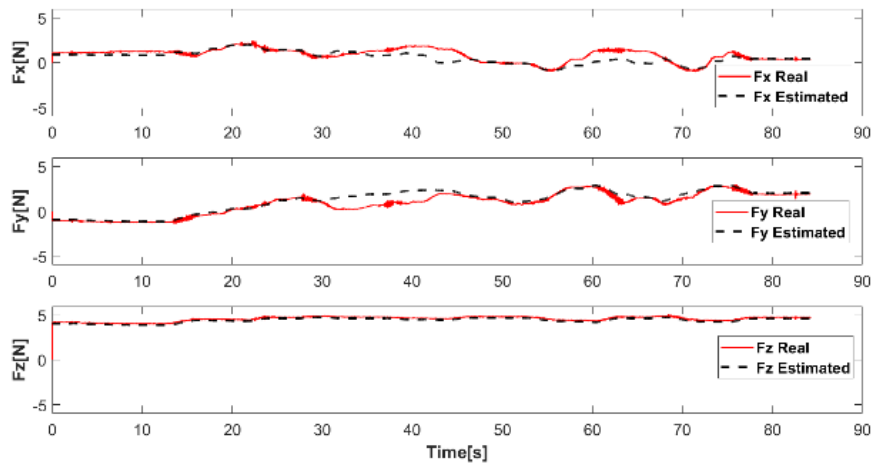


Figure 4.3 Real and Estimated Tool Gravity component with different amount of data.



Figure 4.4 Hand-force applied by medical staff in different poses.

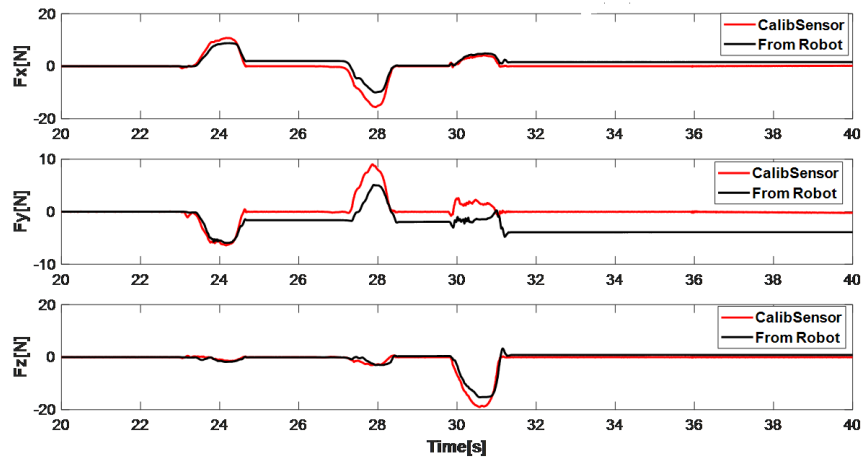


Figure 4.5 Force signals of robot and calibrated sensor.

4.2 Calibration After ANN Implementation

Except for using CF, ANN is also utilized to model the tool gravity force. As reported in Section 3, the number of neurons in hidden is determined by assessing the performances of the regression networks. Hence, we adopt different number of neurons to train several ANN models. For performance evaluation of the trained NN, prediction mean error of swivel angle was calculated, and the root mean square error (RMSE) for prediction of gravity force was calculated as follows:

$$\varepsilon = \sqrt{\frac{\sum_{i=1}^n (\bar{F}_i - \tilde{F}_i)^2}{n}} \quad (4.1)$$

Where \hat{F}_i is the i – th predicted force, and \tilde{F}_i is the i – th measured output force (real value), i is the order of input and output sequences and n is the total sampling number.

The results of the average of obtained three RMSEs on the training and testing datasets are enumerated in Table 4.1, namely:

$$\bar{\varepsilon} = \frac{\varepsilon_x + \varepsilon_y + \varepsilon_z}{3} \quad (4.2)$$

Neurons in Hidden Layer	Training Data (41729)	Testing Data (32047)
	<i>RMSE</i>	<i>RMSE</i>
2	0.4412	0.4248
4	0.3413	0.3758
8	0.0732	0.1065
10	0.0707	0.1042
15	0.0698	0.1035
20	0.0695	0.1039
30	0.0693	0.1030
40	0.0692	0.1116
50	0.0691	0.1118

Table 4.1 Results of network training with different number of neurons in the hidden layer.

In the training procedure, the average of RMSE are reduced along with the increase of the number of neurons in the hidden layer. However, in the testing processing, the changes of mean RMSE reaches to a lowest value (i.e., 0.1030 [N]) when the number of neurons is 30, then becomes worse. This phenomenon is caused by the under-fitting and over-fitting of ANN algorithm. Consequently, the best ANN regression model is the one with 30 neurons in the hidden layer.

Figures 4.6 and 4.7 display predicted force curves by the ANN model (30 neurons) and real forces on the training and testing dataset, respectively.

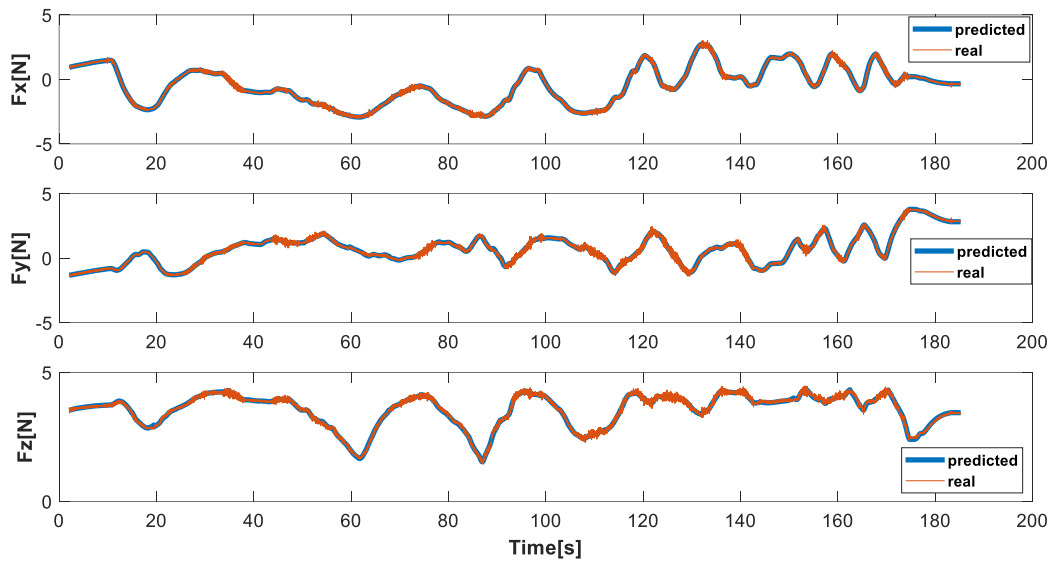


Figure 4.6 The comparison results between the predicted results by ANN model (30 neurons) and the real forces on the training dataset.

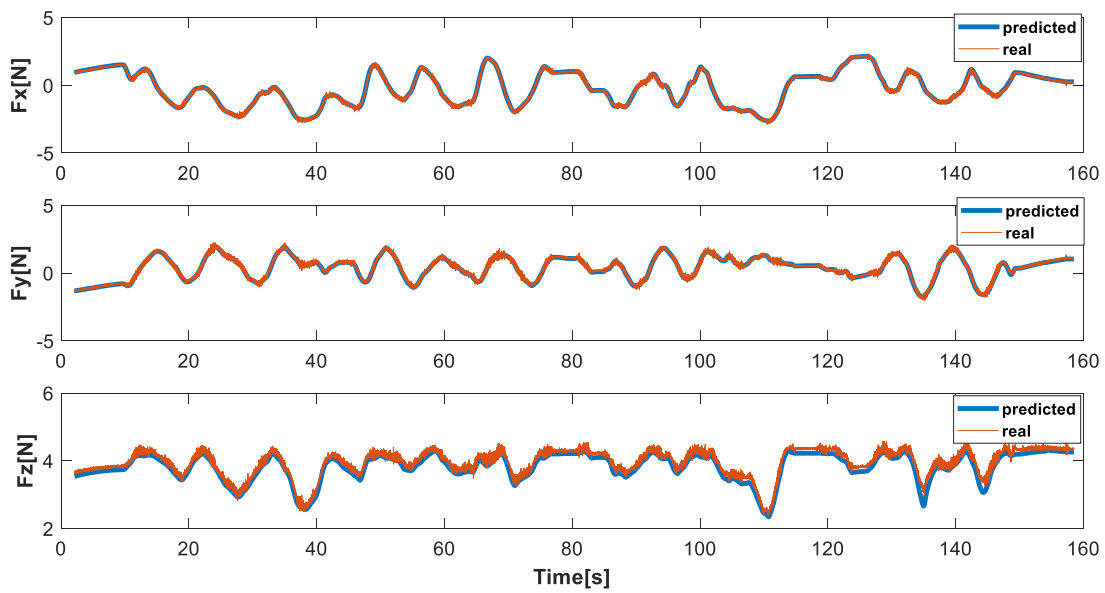


Figure 4.7 The comparison results between the predicted results by ANN model (30 neurons) and the real forces on the testing dataset.

As reported above, after identifying tool gravity component by ANN, we thereafter perform again the force sensor calibration by collecting another data (see 4.4) and then applying the same method SVD. Results of calibration are depicted in Figure 4.8.

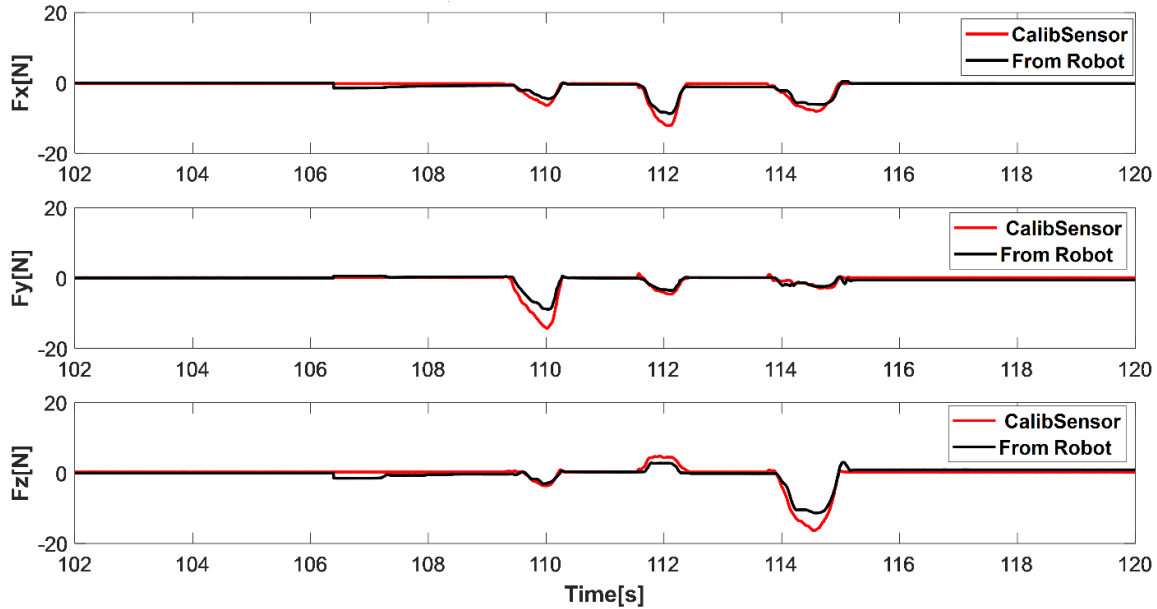


Figure 4.8 Calibration of Force Sensor after tool gravity identification with ANN.

4.3 Discussion

As stated previously, two different techniques were used for tool gravity identification; CF and ANN. Furthermore, force sensor calibration based on SVD method was applied after tool gravity compensation. Repeated verification has been performed to check which is more efficient to be adopted for tool gravity identification. To check the performance, Table 4.2 lists the RMSE of both approaches after tool gravity identification. The 'overall' row is the sum of obtained three RMSEs.

Errors	CF (Fig. 4.3)	NN (Fig. 4.6)
	RMSE [N]	RMSE [N]
E_x	0.552	0.073

E_y	0.525	0.086
E_z	0.156	0.049
Overall	1.233	0.208

Table 4.2 The obtained RMSEs by using CF and ANN (30 neurons) model on the training set.

It is demonstrated that identifying tool gravity component by the ANN (30 neurons) model can obtain high accurate than with CF model. The overall error acquired by ANN model is only 0.208 [N], while CF model is 1.233 [N]. However, the third RMSE is lower than the others because the mathematical model in (3.4) for mapping the z channel force F_z is simpler than the other two channels. It only needs one Euler angle θ_1 , which is easy to be tracked. Similarly, Table 4.4 display the comparison results of RMSE obtained by CF and ANN models on the testing dataset.

Errors	CF (Fig. 4.4)	NN (Fig. 4.7)
	RMSE [N]	RMSE [N]
E_x	1.696	0.079
E_y	2.931	0.096
E_z	1.057	0.134
Overall	5.684	0.309

Table 4.3 The obtained RMSEs by using CF and ANN (30 neurons) model on the training set.

The calibration errors prove that the regression performance on the testing set is worse than training set. Specially, the CF model almost loss the fitting with a overall error 5.684 [N]. The ANN model can also map the Euler angles to the forces with a lower overall RMSE 0.309 [N] which is close to the above results validated on the training set. Although the obtained errors prove that the ANN model (30 neurons) is the best method to predict new forces, the CF model will be a fast method for predicting the forces. Because it has simple regression function and less parameters to calculate. So, if the accuracy is not a compulsory requirement, the CF model can save some computational time for regression.

Attaining the two issues of gravity identification and sensor calibration, this enable to achieve transparency in teleoperated surgery. Figures 4.9 and 4.10 display the performance of bilateral teleoperation. Figure 4.9 shows the force tracking between master and slave devices, where Figure 4.10 show Cartesian positions tracking. It demonstrates that the proposed methodology could achieve transparency in teleoperated surgery.

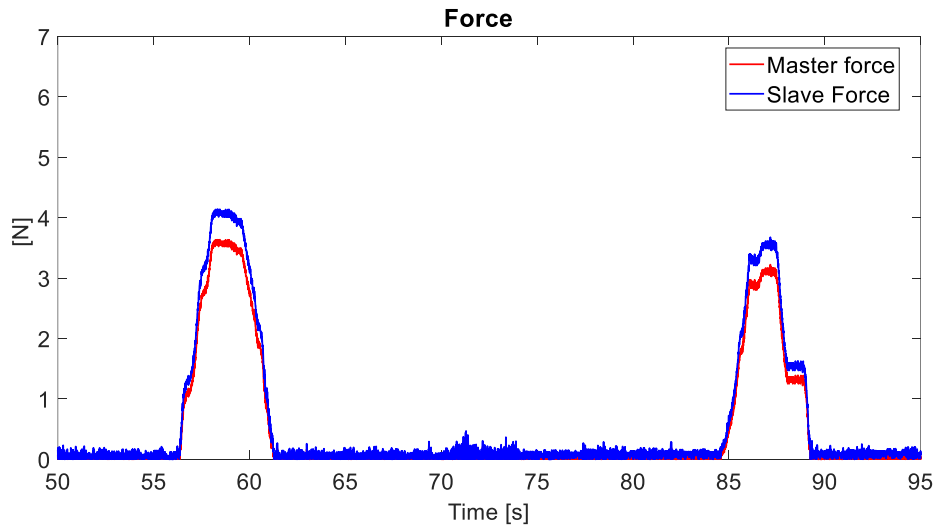


Figure 4.9 Master and Slave Forces during Free Motion and Interaction.

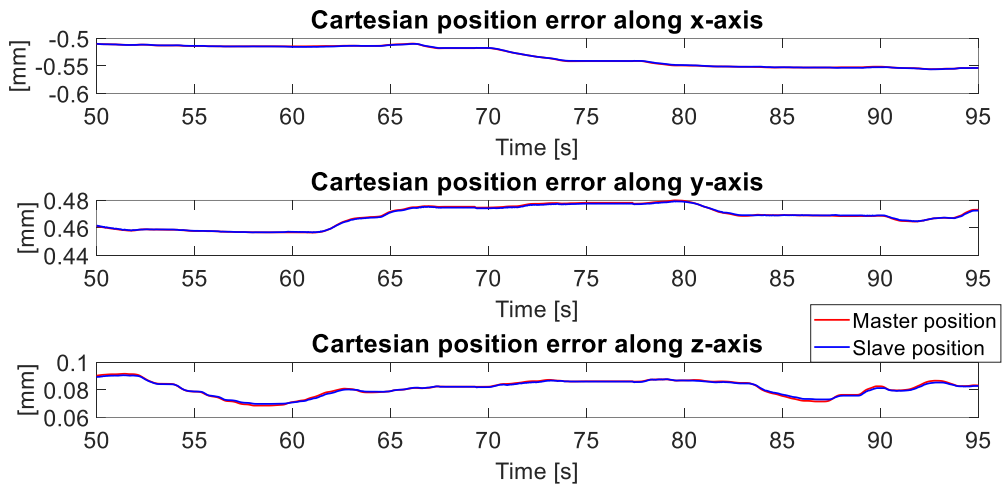


Figure 4.10 Cartesian position errors along 3 axes.

At time where the forces are zero [N], the slave is in free motion ($F_{Interaction} = 0$). When the slave is in contact with environment, the results also demonstrate force and position tracking between master and slave, that are requirements of transparency in Teleoperated surgery.

5. Conclusion and Future Work

The scope of this thesis was to compensate the tool gravity force due to its weight on the force sensor attached to the slave robot's end-effector, in order to reproduce on the master manipulator only the interaction forces of the surgical tool with the tissue. Furthermore, the force sensor must be calibrated in the system where it will be used in order to have accurate measured contact forces to achieve transparency in teleoperation system. Consequently, calibration of the force sensor is adopted so that we can get accurate interaction forces to be felt by the human operator at the local site on the master manipulator. Finally, the two issues were applied on a

serial robot to test the transparency performance of the teleoperation system.

First, while manipulating the force sensor, in the event that is difficult to experience accurate measured values, the slave robot is floating automatically by surgical tool gravity, in spite no manipulation is executed by the surgeon. For this reason,

Tool Gravity Identification aims to estimate the forces exerted on the force sensor by tool's weight during its motion and remove them from the forces measured by the force sensor. Hence, the gravity component must be compensated. To do so, Curve Fitting was adopted to estimate the gravity forces of the surgical, by modelling the mathematical equations of gravity force applied on 3 axes. The result shows that this method was not so efficient and reliable. Besides, Neural Network was developed by using the Toolbox on MATLAB. Using the orientation of the slave's end-effector as an input to the network while the output is the forces measured by the force sensor in free motion and so no interaction was occurred between surgical tool of the slave and the tissue. Results after training the network and validating with other amounts of data, show that this method is so useful to get predicted forces that best fit the real forces measured by the force sensor. By comparison, ANN can model the mapping relations without the prior knowledge of the mathematical model between the orientation angles and the force. However, since it is a non-parametric 'black box', it lacks the knowledge of the dynamics of the system and its accuracy performance maybe worse than the CF which is based on the mathematical model. Furthermore, the comparison errors prove that ANN methods can get a higher accuracy than the CF model. And the ANN model with 30 neurons in the hidden layer is the best model for predicting new forces.

Further, Calibration of force sensor aims to couple force signals of robot and sensor so that we get an accurate force measurement while operating a surgery. The force signals from robot and sensor were collected by applying a hand force on the surgical tool on 3 Cartesian coordinates (x , y , and z) on different poses to validate the calibration. Firstly, the signals show that are in opposite directions, this the sensor must be calibrated in order to have surgical errors on tissue during the surgery. Once the sensor is calibrated using SVD method to get the calibration matrix; it was observed that the two signals after calibration were on the direction, and the surgeon manipulating the master device would feel the real interaction force

experienced by the surgical tool when it touches the tissue at the remote site where the surgical operation is performed.

Results demonstrated that calibration of force sensor after identifying tool gravity component by ANN enhanced robot tool identification and calibration for bilateral teleoperation. In addition, the transparency of the system was achieved by demonstrating force and position tracking of master and slave devices.

Future work will consider more challenging problems (e.g. dead-zone and time-delay) in our bilateral teleoperation control framework. The system stability and tracking accuracy might not be guaranteed under these situations, which are precondition for safety in surgical operation. The work of this thesis does not consider the aspect of stability, which leads to safety of the teleoperated surgery.

Bibliography

- AidanP, & BecharaM. (2017). Gasless trans-axillary robotic thyroidectomy: The introduction and principle.
- BishopM.C., & RoachC. (1992). Fast curve fitting using neural networks. Review of scientific instruments, pg: 4450-4456.
- ChotiprayanakulP., & LiuD. (2009). Workspace mapping and force control for small haptic device based robot teleoperation. International Conference on Information and Automation, (pg 1613-1618).
- De LorenzoDanilo. (2012). Force sensing and display in robotic driven needles for minimally invasive surgery. Milano: NearLab, Politenico di Milano.
- FaberSGert, ChangChien-Chi, Kingmal, SchepersH, HerberS, VeltinkP, & DennerleinJ. (2012). A force plate based method for the calibration of force/torque sensors. Journal of Biomechanics, pg: 1332 – 1338.
- FlorezAJ, & VelasquezA. (2010). Calibration of force sensing resistors (fsr) for static and dynamic applications., (IEEE ANDESCON Conference).
- Force Dimension. (2010). Sigma. 7.: Force Dimension:
<http://www.forcedimension.com/products/sigma-7/overview>
- FrithU, & FrithDC. (1974). Specific motor disabilities in downs syndrome (15). Journal of Child Psychology and Psychiatry.
- GoertzCRaymond, & BevilacquaF. (1952). A force-reflecting positional servomechanism. Nucleonics, pg: 43-45.
- GriffithsG. (2003). Technology and Applications of Autonomous Underwater Vehicles.
- HeckD, SacconA, BeerensR, & NijmeijerH. (2018). Direct Force-Reflecting Two-Layer Approach for Passive Bilateral Teleoperation With Time Delays., (IEEE TRANSACTIONS ON ROBOTICS).

- HirzingerG, SporerN, SchedlM, & ButterfaBJ. (2002). Torque-controlled Light Weight Arms and Articulated Hands - Do We Reach Technological Limits Now?
- HirzingerG, BrunnerB, DietrichJ, & HeindlJ. (1993). Sensor-based space robotics - ROTEX and its telerobotic features.
- Kaushika., SoniA., & SoniR. (1969). A simple neural network approach to software cost estimation. Global Journal of Computer Science and Technology.
- KimK., SunY., VoylesM.R., & NelsonJ.B. (2007). Calibration of multi-axis mems force sensors using the shape-from-motion method. IEEE Sensors Journal, pg: 344-351.
- KuchenbeckerJulianneKatherine. (2006). Characterizing And controlling The High-Frequency Dynamics Of Haptic Interfaces. Stanford University.
- LawrenceADale. (1993). Stability and Transparency in Bilateral Teleoperation., (IEEE TRANSACTIONS ON ROBOTICS AND AUTOMATION).
- LiLarry, CoxBrain, DiftlerMyron, SheltonSusan, & RogersBarry. (1996). Development of a Telepresence Controlled Ambidextrous Robot for Space Applications., (International Conference on Robotics and Automation).
- MamdouhM., & RamadanA.A. (2012). Development of a teleoperation system with a new workspace spanning technique. IEEE International Conference on Robotics and Biomimetics (ROBIO), (pg: 1570-1575).
- MarescauxJ, LeroyJ, GagnerM, RubinoF, MutterD, VixM, . . . SmithM. (2001). Transatlantic robot-assisted telesurgery.
- MarescauxJ, LeroyJ, RubinoF, SmithM, VixM, SimoneM, & MutterD. (2002). Transcontinental robot-assisted remote telesurgery: Feasibility and potential applications. Annals of Surgery.
- MassieHThomas, & SalisburyKennethJ. (1994). The phantom haptic interface: a device for probing virtual objects.
- MassiminoJM, & SheridanBT. (Human factors). Teleoperator performance with varying force and visual feedback. 1994: pg:145-157.
- MurakamiN, ItoA, WillDJ, SteffenM, InoueK, KitaK, & MiyauraS. (2008). Development of a teleoperation system for agricultural vehicles.
- NearLab. (2018). EQUIPMENT.: NearLab: <http://nearlab.polimi.it/medical/equipment/>

- NiemeyerG, PreuscheC, & HirzingerG. (2008). Springer Handbook of Robotics. Springer-Verlan Berlin Heidelberg.
- OkamuraAM. (2004). Methods for haptic feedback in teleoperated robot-assisted surgery. emeraldinsight.
- PacchierottiC, ChinelloF, MalvezziM, MeliL, & PrattichizzoD. (Springer). Two finger grasping simulation with cutaneous and kinesthetic force feedback. 2012: 373-382.
- PapadopouloT., & LourakisI.M. (2000). Estimating the jacobian of the singular value decomposition: Theory and applications., (pg: 554-570).
- PenzaVeronica. (2013). Dynamic Tool Compensation in Bilateral Telemanipulation system for Neurosurgery. Milan: Politecnico di Milano.
- PepeAlberto. (2018). Haptic Device Design and Teleoperation Control Algorithms for Mobile Manipulators. University of Bologna.
- RadiM. (2012). Workspace scaling and haptic feedback for industrial telepresence and teleaction systems with heavy-duty teleoperators. Technical University of Munich.
- RamosA, de Souza BastosE, & KimK.. Obesity and diabetes: .
- RamosA, de Souza BastosEduardo, & KimK. (2015). Obesity and diabetes: New surgical and nonsurgical approaches. Switzerland: Springer International.
- RoobahaniHamid. (2015). Novel contro, haptic and calibration methods for teleoperated electrohydraulic servo systems. Lappeenranta: Lappeenranta University of Technology.
- TalaszAli. (2012). Haptics-Enabled Teleoperation for Robotics-Assisted Minimally Invasive Surgery. The University of Western Ontario.
- TaylorHR, MenciassiA, FichtingerG, FioriniP, & DarioP. (Springer). Medical robotics and computer-integrated surgery. 2016: 1657-1684.
- TobergteA, HelmerP, HagnU, RouillerP, ThielmannS, GrangeS, . . . HirzingerG. (2011). The sigma.7 haptic interface for MiroSurge: A new bi-manual surgical console., (IEEE/RSJ International Conference on Intelligent Robots and Systems).
- TobergteA, KonietschkeR, & HirzingerG. (2009). Planning and control of a teleoperation system for research in minimally invasive robotic surgery., (Robotics and Automationm ICRA, IEEE Interenational Conference).

- TrejosLA, PatelVR, & NaishDM. (2009). Force sensing and its application in minimally invasive surgery and therapy: a survey.
- TrevelyanJ, KangS, & HamelW. (2008). Springer Handbook of Robotics.
- UzunogluE. (2012). position/force control of systems subjected to communication delays and interruptions in bilateral teleoperation. Izmir Institute of Technology.
- WagnerRC, HoweDR, & StylopoulosN. (2002). The role of force feedback in surgery: analysis of blunt dissection. IEEE.
- WenH., MaJ., ZhangM., & MaG. (2012). The comparison research of nonlinear curve fitting in matlab and labview. IEEE Symposium on Electrical & Electronics Engineering (EEESYM), (pg: 74-77).
- YingkunMa, ShilinX, XinongZ, & YajunL. (2012). Hybrid calibration method for six-component force/torque transducers of wind tunnel balance based on support vector machines. Chinese Journal of Aeronautics.

